Hamiltonian spacetime dynamics with a spherical null-dust shell

Jorma Louko*
Department of Physics, University of Maryland, College Park, Maryland 20742-4111

Bernard F. Whiting†
Department of Physics, University of Florida, Gainesville, Florida 32611

John L. Friedman‡
Department of Physics, University of Wisconsin-Milwaukee, P.O. Box 413, Milwaukee, Wisconsin 53201
(Received 7 August 1997; published 16 January 1998)

We consider the Hamiltonian dynamics of spherically symmetric Einstein gravity with a thin null-dust shell, under boundary conditions that fix the evolution of the spatial hypersurfaces at the two asymptotically flat infinities of a Kruskal-like manifold. The constraints are eliminated via a Kuchař-type canonical transformation and Hamiltonian reduction. The reduced phase space $\tilde{\Gamma}$ consists of two disconnected copies of $\mathbb{R}^4$, each associated with one direction of the shell motion. The right-moving and left-moving test shell limits can be attached to the respective components of $\tilde{\Gamma}$ as smooth boundaries with topology $\mathbb{R}^3$. Choosing the right-hand-side and left-hand-side masses as configuration variables provides a global canonical chart on each component of $\tilde{\Gamma}$, and renders the Hamiltonian simple, but encodes the shell dynamics in the momenta in a convoluted way. Choosing the shell curvature radius and the ''interior'' mass as configuration variables renders the shell dynamics transparent in an arbitrarily specifiable stationary gauge ''exterior'' to the shell, but the resulting local canonical charts do not cover the three-dimensional subset of $\tilde{\Gamma}$ that corresponds to a horizon-straddling shell. When the evolution at the infinities is freed by introducing parametrization clocks, we find on the unreduced phase space a global canonical chart that completely decouples the physical degrees of freedom from the pure gauge degrees of freedom. Replacing one infinity by a flat interior leads to analogous results, but with the reduced phase space $\mathbb{R}^2 \cup \mathbb{R}^2$. The utility of the results for quantization is discussed. [S0556-2821(98)03504-8]

PACS number(s): 04.20.Fy, 04.40.Nr, 04.60.Kz, 04.70.Dy

I. INTRODUCTION

Spherically symmetric geometries have a long and useful history as a physically interesting and technically vastly simplified arena for gravitational physics. In vacuum, Einstein's theory with spherical symmetry has no local degrees of freedom, and the reduced phase space in the Hamiltonian formulation is finite dimensional. Including an idealized, infinitesimally thin matter shell brings in an additional finite number of degrees of freedom. Including a continuous matter distribution generically yields a $(1+1)$-dimensional field theory, with the exception of fields whose gauge symmetries exclude spherically symmetric local degrees of freedom. A familiar example of a field with such a gauge symmetry is the electromagnetic field.

In this paper we consider spherically symmetric Einstein gravity coupled to an infinitesimally thin null-dust shell. From the spacetime point of view, the solutions to this system are well known (see, for example, Refs. [1–4]), and they can be easily obtained from a junction condition formalism that is general enough to encompass null shells (see Ref. [5] and the references therein). Our purpose is to explore the Hamiltonian structure of this system, treating both the geometry and the shell as dynamical. Among the extensive previous work on Hamiltonian approaches to spherically symmetric geometries (for a selection in a variety of contexts, see Refs. [6–41]), we follow most closely the canonical transformation techniques of Kuchař [10]. Our main results can be concisely described as generalizing the spherically symmetric vacuum Hamiltonian analysis of Ref. [10] to accommodate a null-dust shell.

Finding a suitable action principle requires care. The shell stress-energy tensor is a delta-distribution with support on the shell history, which is a hypersurface of codimension one. Einstein's equations for the system therefore admit a consistent distributional interpretation [42], and the content of these equations is captured by the junction condition formalism of Barrabes and Israel [5]. We recover these equations from a variational principle. We take the shell action to be that of a spherically symmetric thin cloud of radially-moving massless relativistic point particles, and we vary the total action independently with respect to the gravitational variables and the shell variables. We shall see that this variational principle can be made distributionally consistent and that the variational equations do reproduce the correct dynamics. Achieving this requires, however, a judicious choice

*On leave of absence from Department of Physics, University of Helsinki. Present address: Max-Planck-Institut für Gravitationsphysik, Schlaatzweg 1, D-14473 Potsdam, Germany. Electronic address: louko@aei-potsdam.mpg.de
†Electronic address: bernard@bunyip.phys.ufl.edu
‡Electronic address: friedman@thales.phys.uwm.edu

 © 1998 The American Physical Society

of the regularity properties of the metric.

We begin, in Sec. II, by setting up the Hamiltonian formulation of the system in the Arnowitt-Deser-Misner (ADM) gravitational variables. The spacetime is taken to have Kruskal-like topology, with two asymptotically flat infinities, and the spatial hypersurfaces are taken to be asymptotic to hypersurfaces of constant Killing time at each spacelike infinity. The Killing time evolution of the hypersurfaces is prescribed independently at each infinity. We specify the regularity properties of the gravitational variables, and demonstrate that the variational principle is consistent and leads to the correct equations of motion.

In Sec. III we perform a canonical transformation to a new chart in which the constraints become exceedingly simple. Two of our new variables are Hawking's quasilocal mass $M(r)$ and the two-sphere curvature radius $\mathsf{R}(r)$, just as in the vacuum analysis of Ref. [10]. However, to maintain a consistent distributional interpretation of the variables in the new chart, we are led to relate the momentum conjugate to $M(r)$ to the Eddington-Finkelstein time whose constant value hypersurface coincides with the classical shell history, and not to the Killing time as in Ref. [10]. The momentum conjugate to $\mathsf{R}(r)$ needs to be modified accordingly. Remarkably, the canonical transformation can then be chosen to leave the shell canonical pair invariant. The transformation is mildly singular for geometries in which the shell straddles a horizon, but it can be extended to this special case in a suitable limiting sense.

In Sec. IV we eliminate the constraints by Hamiltonian reduction. The reduced phase space $\widetilde{\Gamma}$ turns out to have dimension four. As the vacuum theory under our boundary conditions has a two-dimensional reduced phase space [10], and as a test shell in a fixed spherically symmetric background has a two-dimensional phase space, this is exactly what one would have anticipated. We first obtain canonical coordinates $(\mathbf{m}_+,\mathbf{m}_-,\mathbf{p}_+,\mathbf{p}_-)$ in which the configuration variables $\mathbf{m}_\pm$ are the Schwarzschild masses on the two sides of the shell. The momenta $\mathbf{p}_\pm$ can be interpreted as the Eddington-Finkelstein time differences between the shell and the infinities, after introducing an appropriate correspondence between our spatial hypersurfaces and hypersurfaces that are asymptotically null. The configuration variables $\mathbf{m}_\pm$ are constants of motion, while the shell motion is indirectly encoded in the dynamics of $\mathbf{p}_\pm$. These coordinates become singular for horizon-straddling shells, but a global chart covering also this special case can be obtained by introducing suitable new momenta. We find that $\widetilde{\Gamma}$ consists of two disconnected copies of $\mathbb{R}^4$, each associated with one direction of the shell motion. The right-moving and left-moving test shell limits, in which the shell stress-energy tensor vanishes, can be attached to the respective components of $\widetilde{\Gamma}$ as smooth boundaries with topology $\mathbb{R}^3$.

In Sec. V we introduce on $\widetilde{\Gamma}$ a local canonical chart in which the shell motion becomes more transparent. Assuming that the shell does not a straddle a horizon, the shell history divides the spacetime into the ''interior,'' which contains a Killing horizon bifurcation two-sphere, and the ''exterior,'' which does not. We choose the configuration variables in the new chart to be the curvature radius of the shell two-sphere and the interior mass, in an arbitrarily specifiable stationary exterior coordinate system. One can argue that this yields a Hamiltonian description of interest for an observer who scrutinizes the shell motion from the exterior asymptotic region, especially if the observer's ignorance of the interior asymptotic region is incorporated by setting the interior contribution to the Hamiltonian to zero. We give three examples of stationary exterior coordinate systems in which the Hamiltonian can be found in closed form. Also, choosing the spatially flat exterior gauge [43–45], and performing a partial reduction by setting the interior mass equal to a prescribed constant, we reproduce the spatially flat shell Hamiltonian previously derived in Refs. [30, 37] by different methods.

In Sec. VI we free the evolution of the spatial hypersurfaces at the spacelike infinities by introducing parametrization clocks. We find on the unreduced phase space a canonical chart in which the physical degrees of freedom and pure gauge degrees of freedom are completely decoupled, in full analogy with the vacuum analysis of Ref. [10]. The pure gauge chart can be chosen so that the configuration variables are the curvature radius of the two-sphere and the Eddington-Finkelstein time, with the latter one appropriately interpreted across the horizons.

In Sec. VII we replace the Kruskal spatial topology $S^2\times\mathbb{R}$ by the spatial topology $\mathbb{R}^3$. The spacetime has then just one asymptotic region, and when the equations of motion hold, the spacetime interior to the shell is flat. As in the Kruskal case, we take the asymptotic region to be asymptotically flat, and we prescribe the evolution of the spatial hypersurfaces at the spacelike infinity. We then carry out the canonical transformation and Hamiltonian reduction. Expectedly, the reduced phase space turns out to consist of two disconnected copies of $\mathbb{R}^2$, with only the counterpart of the pair $(\mathbf{m}_+,\mathbf{p}_+)$ of the Kruskal theory surviving.

We conclude in Sec. VIII with a summary and a brief discussion, including remarks on the potential utility of the results in view of quantization. Some of the technical detail of the ADM dynamical analysis is postponed to the appendices.

We work in Planck units, $\hbar=c=G=1$. Lowercase Latin tensor indices $a,b,\ldots$ are abstract spacetime indices. Dirac's delta-function is denoted by δ, while $\boldsymbol{\delta}$ denotes a variation. The curvature coordinates (T,R) for the Schwarzschild metric are coordinates in which the metric reads

$$ds^2=-(1-2M/R)dT^2+(1-2M/R)^{-1}dR^2+R^2d\Omega^2, \tag{1.1}$$

where $d\Omega^2$ is the metric on the unit two-sphere and M is the Schwarzschild mass. T and R are called respectively the Killing time and the curvature radius.

II. METRIC FORMULATION

In this section we set up the Hamiltonian formulation for spherically symmetric Einstein gravity coupled to a null-dust shell. We pay special attention to the regularity of the gravitational variables and the global boundary conditions.

A. Bulk action

Our spacetime geometry is given by the general spherically symmetric Arnowitt-Deser-Misner (ADM) metric

$$ds^2=-N^2dt^2+\Lambda^2(dr+N^r dt)^2+R^2d\Omega^2, \qquad (2.1)$$

where $d\Omega^2$ is the metric on the unit two-sphere, and N, N^r, Λ, and R are functions of the coordinates t and r only. Partial derivatives with respect to t and r are denoted respectively by overdot and prime, $\dot{}=\partial/\partial t$ and $'=\partial/\partial r$. We take the spacetime metric to be nondegenerate, and N, Λ, and R to be positive.

The matter consists of an infinitesimally thin shell of dust with a fixed total rest mass m, which we initially take to be positive. Denoting the shell history by $r=\mathfrak{r}(t)$, the Lagrangian matter action is

$$S_L^s=-m\int dt\sqrt{\hat{N}^2-\hat{\Lambda}^2(\dot{\mathfrak{r}}+\widehat{N^r})^2}, \qquad (2.2)$$

where a hat is used to denote the value of a variable at the shell. The shell can be envisaged as a thin spherically symmetric cloud of radially-moving massive relativistic point particles.

The Lagrangian gravitational action is obtained by performing integration over the angles in the Einstein-Hilbert action, $(16\pi)^{-1}\int d^4x\sqrt{-g}R$. Discarding a boundary term, the result is [6,7,10,27,30,39]

$$S_L^g=\int dt\int dr[-N^{-1}\{R[\dot{\Lambda}-(\Lambda N^r)'](\dot{R}-R'N^r)+\tfrac{1}{2}\Lambda(\dot{R}-R'N^r)^2\}+N(\Lambda^{-2}RR'\Lambda'-\Lambda^{-1}RR''-\tfrac{1}{2}\Lambda^{-1}R'^2+\tfrac{1}{2}\Lambda)]. \qquad (2.3)$$

The Lagrangian action of the coupled system is

$$S_L=S_L^g+S_L^s+\text{ boundary terms}. \qquad (2.4)$$

We shall consider the regularity properties of the variables, the boundary conditions, and boundary terms after passing to the Hamiltonian formulation.

The momenta conjugate to the configuration variables $\mathfrak{r}$, Λ, and R are

$$\mathfrak{p}=\frac{m\hat{\Lambda}^2(\dot{\mathfrak{r}}+\widehat{N^r})}{\sqrt{\hat{N}^2-\hat{\Lambda}^2(\dot{\mathfrak{r}}+\widehat{N^r})^2}}, \qquad (2.5a)$$

$$P_\Lambda=-\frac{R}{N}(\dot{R}-N^rR'), \qquad (2.5b)$$

$$P_R=-\frac{\Lambda}{N}(\dot{R}-N^rR')-\frac{R}{N}[\dot{\Lambda}-(N^r\Lambda)']. \qquad (2.5c)$$

A Legendre transformation gives the Hamiltonian bulk action [27,30]

$$S_\Sigma=\int dt\left[\mathfrak{p}\dot{\mathfrak{r}}+\int dr(P_\Lambda\dot{\Lambda}+P_R\dot{R}-NH-N^rH_r)\right], \qquad (2.6)$$

where the super-Hamiltonian constraint H and the radial supermomentum constraint H_r contain both gravitational and matter contributions. In the limit $m\to 0$, these constraints take the form

$$H=\frac{\Lambda P_\Lambda^2}{2R^2}-\frac{P_\Lambda P_R}{R}+\frac{RR''}{\Lambda}-\frac{RR'\Lambda'}{\Lambda^2}+\frac{R'^2}{2\Lambda}-\frac{\Lambda}{2}+\frac{\eta\mathfrak{p}}{\Lambda}\delta(r-\mathfrak{r}), \qquad (2.7a)$$

$$H_r=P_RR'-P_\Lambda'\Lambda-\mathfrak{p}\delta(r-\mathfrak{r}), \qquad (2.7b)$$

where $\eta:=\text{sign}(\mathfrak{p})$. From now on, we shall work exclusively in this zero rest mass limit, with the bulk action (2.6) and the constraints (2.7). As will be verified below, the shell then consists of null dust.

The Hamiltonian constraint (2.7a) is not differentiable in $\mathfrak{p}$ at $\mathfrak{p}=0$. As we shall verify below, an initial data set with nonzero $\mathfrak{p}$ cannot evolve into a set with $\mathfrak{p}=0$ [1–5]. We assume from now on that $\mathfrak{p}$ is nonzero: this breaks the phase space into the two disconnected sectors $\eta=\pm 1$. The limits $\mathfrak{p}\to 0_\pm$ within each sector will be addressed in subsection IV C.

B. Local equations of motion

In the presence of a smooth matter distribution, one can assume the spacetime metric to be smooth (C^∞). In the idealized case of an infinitesimally thin shell, the metric can be chosen continuous but not differentiable at the shell [5,42,46,47]. The issue for us is to find smoothness assumptions that give a consistent variational principle. We wish to make both the action (2.6) and its local variations well defined and such that the resulting variational equations are equivalent to Einstein's equations with a null-dust shell.

We follow the massive dust shell treatment of Ref. [37]. In contrast to the case of a massive dust shell, we shall find that the smoothness conditions introduced in Ref. [37] make our null-dust variational principle fully consistent.

As in Ref. [37], we assume that the gravitational variables are smooth functions of r, with the exception that N', $(N^r)'$, Λ', R', P_Λ, and P_R may have finite discontinuities at isolated values of r, and that the coordinate loci of the discontinuities may be smooth functions of t. All the terms under the r-integral in the action (2.6) are well defined in the distributional sense. The most singular contributions are the explicit matter delta-contributions in the constraints, and the implicit delta-functions in R'' and P_Λ'. All these delta-functions are multiplied by continuous functions of r. The remaining terms are at worst discontinuous in r. The action is therefore well defined.

Local independent variations of the action with respect to the gravitational and matter variables give the constraint equations

$$H=0, \qquad (2.8a)$$

$$H_r=0, \qquad (2.8b)$$

and the dynamical equations

$$\dot{\Lambda}=N\left(\frac{\Lambda P_\Lambda}{R^2}-\frac{P_R}{R}\right)+(N^r\Lambda)', \qquad (2.9a)$$

$$\dot{R}=-\frac{NP_\Lambda}{R}+N^rR', \tag{2.9b}$$

$$\dot{P}_\Lambda=\frac{N}{2}\left[-\frac{P_\Lambda^2}{R^2}-\left(\frac{R'}{\Lambda}\right)^2+1+\frac{2\eta\mathfrak{p}}{\Lambda^2}\delta(r-\mathfrak{r})\right]-\frac{N'RR'}{\Lambda^2}+N^rP_\Lambda', \tag{2.9c}$$

$$\dot{P}_R=N\left[\frac{\Lambda P_\Lambda^2}{R^3}-\frac{P_\Lambda P_R}{R^2}-\left(\frac{R'}{\Lambda}\right)'\right]-\left(\frac{N'R}{\Lambda}\right)'+(N^rP_R)', \tag{2.9d}$$

$$\dot{\mathfrak{r}}=\frac{\eta\hat{N}}{\hat{\Lambda}}-\widehat{N^r}, \tag{2.9e}$$

$$\dot{\mathfrak{p}}=\mathfrak{p}\left[\left(N^r-\frac{\eta N}{\Lambda}\right)'\right]\hat{}\,. \tag{2.9f}$$

As will be discussed in detail in Appendix A, our smoothness conditions imply that equations (2.8) and all save the last one of equations (2.9) have an unambiguous distributional interpretation. Equation (2.9f), on the other hand, is ambiguous: the right-hand side is a combination of spatial derivatives evaluated at the shell, but these derivatives may be discontinuous. We need to examine the dynamical content of the well-defined equations, and the possibilities of interpreting equation (2.9f).

A first observation from equation (2.9e) is that the shell history is tangent to the null vector ℓ^a whose components are

$$\ell^t=1, \tag{2.10a}$$

$$\ell^r=\eta\hat{N}\hat{\Lambda}^{-1}-\widehat{N^r}. \tag{2.10b}$$

For $\eta=1$ ($\eta=-1$), ℓ^a is the future null vector that points towards relatively larger (smaller) values of r. From the definition of the shell stress-energy tensor, $\delta_g S_{\rm shell}=\frac{1}{2}\int\sqrt{-g}d^4xT^{ab}\delta(g_{ab})$, we find

$$T^{ab}=\frac{\eta\mathfrak{p}}{4\pi N^2\Lambda^2R^2}\ell^a\ell^b\delta(r-\mathfrak{r}). \tag{2.11}$$

The shell is therefore null, with positive surface energy but vanishing surface pressure [5]. This confirms that the shell consists of null dust.

All solutions to the spherically symmetric Einstein equations with a null-dust shell can be found from a sufficiently general junction condition formalism [1–5]. On each side of the shell, the spacetime is locally part of the extended Schwarzschild geometry. If the global structure of the spacetime is Kruskal-like, with two asymptotically flat infinities, there are only two qualitatively different cases. First, if the shell is not static, the junction is completely determined by continuity of the two-sphere radius at the shell. The motion is clearly geodesic in each of the two geometries, and the radius of the two-sphere serves as an affine parameter in either geometry. The spacetime is either that shown in Fig. 1, or its time and/or space inverse. Second, if the shell is static, the junction is along a common horizon, and the masses must agree. The soldering is affine, meaning that the affine parameters along the horizon with respect to the two geometries are affinely related; however, as the stress-energy tensor of the shell is by assumption nonvanishing, the bifurcation two-spheres on the two sides do not coincide. The spacetime is either that shown in Fig. 2 or its time inverse.

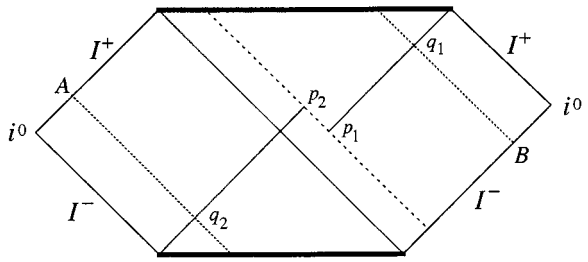

FIG. 1. The Penrose diagram for a spacetime in which the shell does not straddle a horizon. The shell history is the dashed line passing through points p_1 and p_2. The shell has been taken left-moving, which means $\eta=-1$, and to lie in the future of the left-going horizon, which means that the right-hand-side Schwarzschild mass $\mathbf{m}_+$ is greater than the left-hand-side Schwarzschild mass $\mathbf{m}_-$. The diagrams for $\eta=1$ and/or $\mathbf{m}_+<\mathbf{m}_-$ are obtained through inversions of space or time or both. The spacetime is uniquely determined by the values of $\mathbf{m}_+$, $\mathbf{m}_-$, and η. A hypersurface of constant t extends from the left-hand-side i^0 to the right-hand-side i^0, and the points A and B indicate the ends of the asymptotically null hypersurface introduced in Sec. IV. The dotted lines are hypersurfaces of constant null time ending respectively at A and B. Point B is here shown as being in the future of the shell history, but in general it could be anywhere on the right-hand-side $\mathcal{I}^-$.

Now, away from the shell, equations (2.8) and (2.9) are well known to be equivalent to Einstein's equations. We shall investigate equations (2.8) and (2.9) at the shell in detail in the appendices. The result is that, when combined with the fact that the geometry is locally Schwarzschild on each side of the shell, the well-defined equations, (2.8) and (2.9a)–(2.9e), are equivalent to the correct null-dust junction conditions at the shell. They further imply that the right-hand side of (2.9f) is unambiguous, and that (2.9f) is satisfied as an identity. Our variational principle is therefore consistent, and it correctly reproduces the motion of a null-dust shell.

A check on the consistency of our formalism is that the Poisson brackets of our constraints can be shown to obey the radial hypersurface deformation algebra [48], as in the ab-

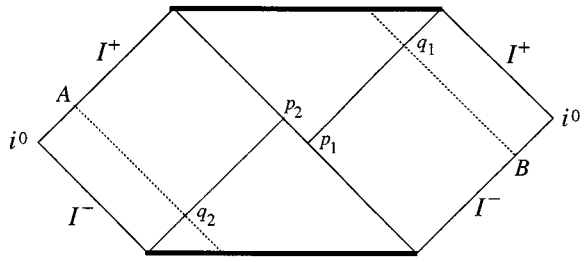

FIG. 2. The Penrose diagram for a spacetime in which the shell straddles a horizon. The shell history is the line passing through points p_1 and p_2. The spacetimes on the two sides share a common Schwarzschild mass $\mathbf{m}$. The shell has been taken left-moving, which means $\eta=-1$. The diagram corresponding to $\eta=1$ is obtained through time (or, equivalently, space) inversion. The spacetime is uniquely determined by the values of $\mathbf{m}$ and η. The points A and B and the dotted null lines ending at them are as in Fig. 1.

sence of the shell, and as with a massive dust shell [37]. We therefore have a Hamiltonian system with first class constraints [49].

C. Falloff

What remains are the global boundary conditions. We take the coordinate r to have the range $(-\infty,\infty)$, and as $r \to \pm\infty$ we assume the falloff [10,50]

$$\Lambda(t,r)=1+M_{\pm}|r|^{-1}+O^{\infty}(|r|^{-1-\epsilon}), \tag{2.12a}$$

$$R(t,r)=|r|+O^{\infty}(|r|^{-\epsilon}), \tag{2.12b}$$

$$P_{\Lambda}(t,r)=O^{\infty}(|r|^{-\epsilon}), \tag{2.12c}$$

$$P_{R}(t,r)=O^{\infty}(|r|^{-1-\epsilon}), \tag{2.12d}$$

$$N(t,r)=N_{\pm}+O^{\infty}(|r|^{-\epsilon}), \tag{2.12e}$$

$$N^{r}(t,r)=O^{\infty}(|r|^{-\epsilon}), \tag{2.12f}$$

where $M_{\pm}$ and $N_{\pm}$ are functions of t, and ϵ is a parameter that can be chosen freely in the range $0<\epsilon\leqslant 1$. Here, O^{∞} stands for a term that falls off as $r\to\pm\infty$ as its argument, and whose derivatives with respect to r and t fall off accordingly. These conditions imply that the asymptotic regions associated with $r\to\pm\infty$ are asymptotically flat, with the constant t hypersurfaces asymptotic to hypersurfaces of constant Minkowski time. $N_{\pm}$ are the rates at which the asymptotic Minkowski times evolve with respect to the coordinate time t. When the equations of motion hold, $M_{\pm}$ are time-independent and equal to the Schwarzschild masses.

In the variational principle, we take $N_{\pm}$ to be prescribed functions of t, but leave $M_{\pm}$ free. The appropriate total action then reads [10]

$$S=S_{\Sigma}+S_{\partial\Sigma}, \tag{2.13a}$$

where the boundary action is

$$S_{\partial\Sigma}=-\int dt(N_{+}M_{+}+N_{-}M_{-}). \tag{2.13b}$$

The global structure of the spacetime is Kruskal-like, with two asymptotically flat asymptotic regions. The classical solutions under these boundary conditions are precisely those described above and shown in Figs. 1 and 2.

III. CANONICAL TRANSFORMATION

In this section we find a new canonical chart in which the constraints become exceedingly simple. Away from the shell, our treatment closely follows that given by Kuchař in the vacuum case [10]. The new elements arise mainly from patching the two vacuum regions together at the shell.

Our canonical transformation turns out to be mildly singular when the masses on the two sides of the shell agree and the shell straddles a common horizon. We first perform the transformation, in subsection III A, assuming that this special case has been excluded. We then argue, in subsection III B, that the transformation can be extended to the special case in a suitable limiting sense.

A. Shell not on a horizon

In the vacuum theory, Kuchař [10] found a transformation from the canonical chart $(\Lambda,R,P_{\Lambda},P_{R})$ to the new canonical chart $(M,\mathsf{R},P_{M},P_{\mathsf{R}})$ defined by

$$M:=\tfrac{1}{2}R(1-F), \tag{3.1a}$$

$$\mathsf{R}:=R, \tag{3.1b}$$

$$P_{M}:=R^{-1}F^{-1}\Lambda P_{\Lambda}, \tag{3.1c}$$

$$P_{\mathsf{R}}:=P_{R}-\tfrac{1}{2}R^{-1}\Lambda P_{\Lambda}-\tfrac{1}{2}R^{-1}F^{-1}\Lambda P_{\Lambda} -R^{-1}\Lambda^{-2}F^{-1}[(\Lambda P_{\Lambda})'(RR')-(\Lambda P_{\Lambda})(RR')'], \tag{3.1d}$$

where

$$F:=\left(\frac{R'}{\Lambda}\right)^{2}-\left(\frac{P_{\Lambda}}{R}\right)^{2}. \tag{3.2}$$

When the equations of motion hold, M is independent of both r and t, and its value is just the Schwarzschild mass. Similarly, when the equations of motion hold, we have $P_{M}=-T'$, where T is the Killing time. The vacuum constraints can be written as a linear combination of M' and P_{R}, and the dynamical content of the theory becomes transparent.

In the presence of our null shell, the variables $(M,\mathsf{R},P_{M},P_{\mathsf{R}})$ become singular at the shell. To see this, consider a classical solution in which the shell history does not lie on a horizon. As M is discontinuous at the shell, $\dot{M}$ contains at the shell a delta-function in r. As P_{M} is discontinuous at the shell, the product $P_{M}\dot{M}$ is ambiguous. One therefore does not expect the chart $(M,\mathsf{R},P_{M},P_{\mathsf{R}})$ to be viable in the presence of the shell.

To overcome this difficulty, we keep M and R but replace the momenta by ones that are smoother across the shell. We define first [10]

$$F_{\pm}:=\frac{R'}{\Lambda}\pm\frac{P_{\Lambda}}{R} \tag{3.3}$$

and

$$F_{\pm\eta}:=\frac{R'}{\Lambda}\pm\eta\frac{P_{\Lambda}}{R}. \tag{3.4}$$

Note that $F=F_{+}F_{-}=F_{\eta}F_{-\eta}$. When the equations of motion hold, F_{+} vanishes on the leftgoing branch(es) of the horizon and F_{-} vanishes on the rightgoing branch(es) of the horizon. It follows that $F_{-\eta}$ is nonvanishing on the horizon that the shell crosses. Now let

$$\Pi_{M}:=P_{M}+\eta F^{-1}R'=\eta\Lambda F_{-\eta}^{-1}, \tag{3.5a}$$

$$\Pi_{\mathsf{R}}:=P_{\mathsf{R}}-\eta F^{-1}M'=P_{R}+\eta R(\ln|F_{-\eta}|)'+\frac{\eta\Lambda}{2}(F_{-\eta}-F_{-\eta}^{-1}). \tag{3.5b}$$

When the equations of motion hold, equation (3.5a) shows that

$$\Pi_M = -(T - \eta r^*)', \tag{3.6}$$

where r^* is the tortoise coordinate [47]. For $\eta = +1$ ($\eta = -1$), $T - \eta r^*$ is the retarded (advanced) Eddington-Finkelstein time coordinate. While P_M was associated with the Killing time [10], our prospective new momentum Π_M is therefore associated with the retarded or advanced Eddington-Finkelstein time.

Away from the shell, a calculation of the Poisson brackets shows that the set $(M, \mathsf{R}, \Pi_M, \Pi_{\mathsf{R}})$ is a candidate for a new gravitational canonical chart. We need to find shell variables that complete this set into a full canonical chart.

For the rest of this subsection, we assume that the shell history does not lie on a horizon. The special case where the shell straddles a horizon will be discussed in subsection III B.

As a preliminary, suppose that the constraints (2.8) hold, and consider the regularity of the variables. Away from the shell, the constraints (2.8) imply that R' and P_Λ are continuous, and $F_\pm$ are thus both continuous. In the notation of appendix A, the distributional content (A2) of the constraints at the shell can be written as

$$0 = \Delta F_{-\eta}, \tag{3.7a}$$

$$0 = \mathfrak{p} + \Delta(\Lambda P_\Lambda). \tag{3.7b}$$

From (3.7a) we see that $F_{-\eta}$ is continuous at the shell. Equation (3.5a) then implies that Π_M is continuous, with the exception that it diverges on the horizon that is parallel to the shell history. The first equality sign in (3.5b), and the observation that the vacuum constraints are linear combinations of M' and P_{R} [10], imply that Π_{R} is vanishing everywhere except possibly at the shell. The rightmost expression in (3.5b) shows that Π_{R} cannot contain a delta-function at the shell, and Π_{R} is therefore everywhere vanishing. From now on, we can therefore proceed assuming that $F_{-\eta}$ and Π_{R} are continuous, and that their r-derivatives have at most finite discontinuities at isolated values of r. By (3.5a), the same will then hold for Π_M, with the exception of the horizon where Π_M diverges. This tightens the neighborhood of the classical solutions in which the fields can take values, but it will not affect the critical points of the action. The reason for this assumption is that it will make the terms $\Pi_M \dot{M}$ and $\Pi_{\mathsf{R}} \dot{\mathsf{R}}$ in our new action distributionally well defined.

We can now proceed to the Liouville forms. A direct computation yields

$$\begin{aligned} P_\Lambda \boldsymbol{\delta}\Lambda + P_R \boldsymbol{\delta} R + M \boldsymbol{\delta}\Pi_M - \Pi_{\mathsf{R}} \boldsymbol{\delta}\mathsf{R} \\ = -(\eta R \boldsymbol{\delta} R \ \ln|F_{-\eta}|)' + \boldsymbol{\delta}\left[\frac{\eta R \Lambda}{2} (F_{-\eta}^{-1} - F_{-\eta}) \right. \\ \left. + \eta R R' \ \ln|F_{-\eta}| \right]. \end{aligned} \tag{3.8}$$

The variation $\boldsymbol{\delta}$ affects the smoothness of the gravitational variables in the same way as the time derivative in subsection II B. Away from the horizon parallel to the shell history, on which $F_{-\eta}$ vanishes and Π_M diverges, all the terms in (3.8) are therefore distributionally well defined: the terms on the left-hand side are at most discontinuous in r, while the terms on the right-hand side may contain at worst delta-functions arising from $(\boldsymbol{\delta} R)'$. The status at the horizon on which $F_{-\eta}$ vanishes will be discussed below.

To obtain the difference in the prospective Liouville forms, we need to integrate the relation (3.8) over r. In an integral over a finite interval in r, the only subtlety arises from the horizon on which $F_{-\eta}$ vanishes. On a classical solution with mass M, it can be shown from the embedding analysis of Appendix C that

$$F_{-\eta} = \frac{\Lambda_h}{4M}(r - r_h) + O((r - r_h)^2), \tag{3.9}$$

where the subscript h indicates the values of the quantities at the horizon on which $F_{-\eta}$ vanishes. Equations (3.9) and (3.5a) therefore show that, on the classical solution, the integral of (3.8) across the horizon is well defined in the principal value sense, just as in the corresponding analysis of Ref. [10]. To extend this argument off the classical solutions, we note that when the constraints hold, $M(r)$ is constant in r across this horizon. As our action contains the constraints with their associated Lagrange multiplies, we argue that $M(r)$ can be assumed smooth at the horizon in the relation (3.8). We can then again employ (3.9) and (3.5a), and it is seen as above that the integral of (3.8) across this horizon is well defined in the principal value sense.

What needs more attention is the falloff in (3.8) at the infinities. From (2.12), (3.1), and (3.5), we have

$$M(t,r) = M_\pm(t) + O^\infty(|r|^{-\epsilon}), \tag{3.10a}$$

$$\mathsf{R}(t,r) = |r| + O^\infty(|r|^{-\epsilon}), \tag{3.10b}$$

$$\Pi_M(t,r) = \pm\eta(1 + 2M_\pm|r|^{-1}) + O^\infty(|r|^{-1-\epsilon}), \tag{3.10c}$$

$$\Pi_{\mathsf{R}}(t,r) = O^\infty(|r|^{-1-\epsilon}). \tag{3.10d}$$

This means that the integrals of the third term on the left-hand side and the total variation term on the right-hand side diverge as $r \to \pm\infty$. The geometrical reason for this divergence is, as seen from (3.6), that Π_M is associated with a *null* time, rather than an asymptotically Minkowski time.

The cure is to introduce convergence functions that provide the necessary translation between asymptotically spacelike hypersurfaces and asymptotically null hypersurfaces. To this end, let $g(M_+, M_-; r)$ be a function that is smooth in r and depends on our variables only through M_+ and M_- as indicated. Let g have the falloff

$$g(M_+, M_-; r) = \pm M_\pm^2 |r|^{-1} + O^\infty(|r|^{-1-\epsilon}). \tag{3.11}$$

Adding $-\eta \boldsymbol{\delta} g$ on both sides of (3.8) yields now an equation whose both sides can be integrated in r from $-\infty$ to ∞. The substitution terms arising from the first term on the right-hand side vanish, and we obtain

$$\int_{-\infty}^{\infty}(P_\Lambda \boldsymbol{\delta}\Lambda + P_R \boldsymbol{\delta} R)dr = \int_{-\infty}^{\infty}(\Pi_{\mathsf{R}}\boldsymbol{\delta}\mathsf{R} - M\boldsymbol{\delta}\Pi_M + \eta\boldsymbol{\delta}g)dr + \boldsymbol{\delta}\left\{\int_{-\infty}^{\infty}\left[\frac{\eta R\Lambda}{2}(F_{-\eta}^{-1} - F_{-\eta}) + \eta R R' \ln|F_{-\eta}| - \eta g\right]dr\right\}. \tag{3.12}$$

All the terms in (3.12) are well defined, provided the integral across the horizon on which $F_{-\eta}$ vanishes is interpreted in the principal value sense. We therefore see that the set $(M,\mathsf{R},\mathfrak{r},\Pi_M,\Pi_{\mathsf{R}},\mathfrak{p})$ provides a new canonical chart on the phase space. Note that this canonical transformation leaves the shell variables $(\mathfrak{r},\mathfrak{p})$ entirely invariant. The geometrical meaning of the convergence function g will be discussed in Sec. IV.

What remains is to write the constraint terms in the action in terms of the new variables. Consider first the constraints away from the shell. A straightforward rearrangement yields

$$NH + N^r H_r = N^{\mathsf{R}}\Pi_{\mathsf{R}} + \widetilde{N}M', \tag{3.13}$$

where

$$\widetilde{N} := (\eta\Lambda N^r - N)F_{-\eta}^{-1}, \tag{3.14a}$$

$$N^{\mathsf{R}} := N^r R' - NR^{-1}P_\Lambda. \tag{3.14b}$$

Note that N^{R} is the same as in Ref. [10]. Both terms on the right-hand side of (3.13) are distributionally well defined. Away from the shell, we can therefore include the constraints in the action in the form shown on the right-hand side of (3.13), with $\widetilde{N}$ and N^{R} as independent Lagrange multipliers. This constraint redefinition is mildly singular on the horizon parallel to the shell history, owing to the divergence of Π_M; however, one can argue as in Ref. [10] that the redefined constraints are equivalent to the old ones by continuity. The falloff of the new multipliers is

$$\widetilde{N} = \mp N_\pm + O^\infty(|r|^{-\epsilon}), \tag{3.15a}$$

$$N^{\mathsf{R}} = O^\infty(|r|^{-\epsilon}). \tag{3.15b}$$

To recover the delta-constraint (3.7a), we observe from (3.5b) that (3.7a) is equivalent to Π_{R} not having a delta-contribution at the shell. We therefore argue that including in the action the constraint term $-\int dt\int_{-\infty}^{\infty}dr N^{\mathsf{R}}\Pi_{\mathsf{R}}$, with N^{R} an independent Lagrange multiplier, yields both the constraint $\Pi_{\mathsf{R}}=0$ away from the shell and the delta-constraint (3.7a) at the shell.[1]

Finally, consider the delta-constraint (3.7b). Using (3.5a) and (3.7a), equation (3.1a) implies

$$\Delta M = -\frac{\Delta(\Lambda P_\Lambda)}{\widehat{\Pi_M}}. \tag{3.16}$$

When (3.7a) holds, (3.7b) is thus equivalent to

$$\Delta M = \frac{\mathfrak{p}}{\widehat{\Pi_M}}. \tag{3.17}$$

Including in the action the constraint term $-\int dt\int_{-\infty}^{\infty}dr\widetilde{N}[M' - \mathfrak{p}\Pi_M^{-1}\delta(r-\mathfrak{r})]$, with $\widetilde{N}$ an independent Lagrange multiplier, therefore yields both the constraint $M'=0$ away from the shell and the delta-constraint (3.7b) at the shell.

These considerations have led us to the action

$$S = \int dt\left[\mathfrak{p}\dot{\mathfrak{r}} + \int_{-\infty}^{\infty}dr(\Pi_{\mathsf{R}}\dot{\mathsf{R}} - M\dot{\Pi}_M + \eta\dot{g})\right] - \int dt\int_{-\infty}^{\infty}dr\{N^{\mathsf{R}}\Pi_{\mathsf{R}} + \widetilde{N}[M' - \mathfrak{p}\Pi_M^{-1}\delta(r-\mathfrak{r})]\} - \int dt(N_+M_+ + N_-M_-). \tag{3.18}$$

Both the action and its variations are well defined. The Poisson bracket algebra of the constraints clearly closes. Note that the convergence term $\eta\dot{g}$ in no way contributes to the local variations of the action.

The Liouville term $-M\dot{\Pi}_M$ can be brought to a form in which the time derivative is on M, at the cost of introducing another convergence term. Let $G(r)$ be a smooth function of r only, with the falloff

$$G(r) = \pm 1 + O^\infty(|r|^{-1-\epsilon}). \tag{3.19}$$

We then have

$$\eta\dot{g} - M\dot{\Pi}_M = (\Pi_M - \eta G)\dot{M} - \eta\dot{g} + \frac{d}{dt}(\eta GM + 2\eta g - M\Pi_M). \tag{3.20}$$

All the terms in (3.20) are well defined, and each side can be integrated in r from $-\infty$ to ∞. We arrive at the action

$$S = \int dt\left\{\mathfrak{p}\dot{\mathfrak{r}} + \int_{-\infty}^{\infty}dr[\Pi_{\mathsf{R}}\dot{\mathsf{R}} + (\Pi_M - \eta G)\dot{M} - \eta\dot{g}]\right\} - \int dt\int_{-\infty}^{\infty}dr\{N^{\mathsf{R}}\Pi_{\mathsf{R}} + \widetilde{N}[M' - \mathfrak{p}\Pi_M^{-1}\delta(r-\mathfrak{r})]\} - \int dt(N_+M_+ + N_-M_-). \tag{3.21}$$

The geometrical meaning of the convergence terms will become explicit in Sec. IV.

[1] A subtlety in this argument is that N^{R} need not be continuous at the shell, not even on the classical solutions. The product $N^{\mathsf{R}}\Pi_{\mathsf{R}}$ would therefore not be distributionally well defined in the event that Π_{R} did contain a delta-contribution at the shell.

B. Shell on a horizon

In subsection III A we excluded the special case where the shell straddles a horizon. We now discuss how this special case can be included.

When the shell straddles a horizon, the zero of $F_{-\eta}$ occurs at the shell. The delta-constraints at the shell are given by (3.7). When the equations of motion hold, the masses on the two sides agree, and the embedding analysis of Appendix C shows that equation (3.9) holds, now with $\Lambda_h=\hat{\Lambda}$ and $r_h=\mathfrak{r}$. From (3.5b) we see that Π_{R} cannot contain a delta-function at the shell. We can therefore again assume that $F_{-\eta}$ and Π_{R} are continuous, and that their r-derivatives have at most finite discontinuities at isolated values of r.

The new feature in equation (3.8) is that the singularity of $F_{-\eta}^{-1}$ and Π_M now occurs at the shell. When the equations of motion hold, we see from (3.5a) and (3.9) that integrating each side of (3.8) in r across the shell is well defined in the principal value sense, and we argue as above that this conclusion can be extended away from the classical solutions provided the constraints are understood to hold. We argue similarly that the left-hand side of (3.8) contains no delta-contributions at the shell, and it is therefore justified to interpret the integral of (3.8) over r as the principal value. Convergence at the infinities is accomplished as above, and the substitution terms from the total r-derivative on the right-hand side of (3.8) vanish. We therefore again arrive at (3.12). Equations (3.16) and (3.17) remain valid, with the understanding $(\widehat{\Pi_M})^{-1}=0$, and the delta-constraints can be taken in the action as before. To justify the manipulations leading to the action (3.21), we again appeal to the constraints to argue that M can be regarded as smooth in r at the shell, and that $\dot{M}$ then does not contain a delta-function at the shell.

We therefore see that the actions (3.18) and (3.21) remain valid in a suitable limiting sense also for a horizon-straddling shell.

IV. REDUCTION

In this section we eliminate the constraints and find the dynamics in the reduced phase space. We shall continue to treat the cases $\eta=\pm 1$ separately, and we denote the corresponding two components of the reduced phase space by $\widetilde{\Gamma}_\eta$. We first assume, in subsection IV A, that the shell history does not lie on a horizon, and we then include the horizon-straddling shell as a limiting case in subsection IV B. Finally, in subsection IV C, we attach the right-moving and left-moving test shell limits to the respective components of the reduced phase space as regular boundaries.

It will be useful in the reduction to assume a more definite form for the convergence function g. From now on, we take

$$g(M_+,M_-;r)=M_+^2 g_+(r)+M_-^2 g_-(r), \tag{4.1a}$$

where $g_\pm(r)$ are smooth functions of r only, with the falloff

$$g_\pm(r)=\pm|r|^{-1}\theta(\pm r)+O^\infty(|r|^{-1-\epsilon}), \tag{4.1b}$$

where θ denotes the step function.

A. Shell not on a horizon

In this subsection we assume that the shell history does not lie on a horizon.

Solving the constraint $\Pi_{\mathsf{R}}=0$ implies that R and Π_{R} simply drop out of the action. To solve the remaining constraint,

$$\Pi_M M'-\mathfrak{p}\,\delta(r-\mathfrak{r})=0, \tag{4.2}$$

we write

$$M=\mathbf{m}_+\,\theta(r-\mathfrak{r})+\mathbf{m}_-\,\theta(\mathfrak{r}-r), \tag{4.3}$$

where $\mathbf{m}_\pm(t)$ are regarded as independent variables. We then have

$$\dot{M}(r)=\dot{\mathbf{m}}_+\,\theta(r-\mathfrak{r})+\dot{\mathbf{m}}_-\,\theta(\mathfrak{r}-r)+(\mathbf{m}_--\mathbf{m}_+)\dot{\mathfrak{r}}\,\delta(r-\mathfrak{r}), \tag{4.4}$$

and the constraint (4.2) implies

$$\mathfrak{p}=(\mathbf{m}_+-\mathbf{m}_-)\widehat{\Pi_M}. \tag{4.5}$$

Note that as the shell history does not lie on a horizon, each of the two factors on the right-hand side of (4.5) is nonvanishing.

Using (4.1b), (4.4), and (4.5), we find

$$\mathfrak{p}\dot{\mathfrak{r}}+\int_{-\infty}^{\infty}dr[(\Pi_M-\eta G)\dot{M}-\eta\dot{g}]=\mathbf{p}_+\dot{\mathbf{m}}_++\mathbf{p}_-\dot{\mathbf{m}}_-+\frac{d}{dt}\left[\eta(\mathbf{m}_+-\mathbf{m}_-)\times\int_0^{\mathfrak{r}}G\,dr\right], \tag{4.6}$$

where

$$\mathbf{p}_+:=\int_{-\infty}^{\infty}dr[\Pi_M\theta(r-\mathfrak{r})-\eta G\,\theta(r)-2\,\eta\mathbf{m}_+g_+], \tag{4.7a}$$

$$\mathbf{p}_-:=\int_{-\infty}^{\infty}dr[\Pi_M\theta(\mathfrak{r}-r)-\eta G\,\theta(-r)-2\,\eta\mathbf{m}_-g_-]. \tag{4.7b}$$

The singularity of $\Pi_M(r)$ occurs in precisely one of the two integrals in (4.7), and the integral over this singularity is interpreted in the principal value sense. Substituting (4.6) into (3.21), and dropping the integral of a total derivative, we obtain the reduced action

$$S=\int dt(\mathbf{p}_+\dot{\mathbf{m}}_++\mathbf{p}_-\dot{\mathbf{m}}_--N_+\mathbf{m}_+-N_-\mathbf{m}_-). \tag{4.8}$$

This shows that the set $(\mathbf{m}_+,\mathbf{m}_-,\mathbf{p}_+,\mathbf{p}_-)$ provides local canonical coordinates on $\widetilde{\Gamma}_\eta$. The equations of motion derived from the action (4.8) read

$$\dot{\mathbf{m}}_\pm=0, \tag{4.9a}$$

$$\dot{\mathbf{p}}_\pm=-N_\pm \tag{4.9b}$$

The emergence of $\mathbf{m}_\pm$ as two coordinates on $\tilde{\Gamma}_\eta$ is not surprising: on a classical solution, $\mathbf{m}_\pm$ are the two Schwarzschild masses, and these masses together with η completely determine the four-dimensional spacetime. To understand the geometrical meaning of $\mathbf{p}_\pm$, we recall from (3.6) that without the convergence terms proportional to G and $g_\pm$, the integrals in (4.7) would give the Eddington-Finkelstein time differences between the shell and the infinities on the constant t hypersurface. As the constant t hypersurface extends to the spacelike infinities, such null-time differences would be infinite. The role of the convergence terms in (4.7) is to absorb the infinities: one can think of the convergence terms as associating to the constant t hypersurface a hypersurface that is asymptotically *null* as $r\to\pm\infty$. For $\eta=-1$, this associated hypersurface extends from the left-hand-side $\mathcal{I}^+$ to the right-hand-side $\mathcal{I}^-$ (points A and B in Fig. 1); for $\eta=1$, the situation is the reverse. Thus, $\mathbf{p}_+$ is the Eddington-Finkelstein time difference between the shell and the right-hand-side infinity of the associated asymptotically null hypersurface, and $-\mathbf{p}_-$ is the Eddington-Finkelstein time difference between the shell and the left-hand-side infinity of the associated asymptotically null hypersurface. The equations of motion (4.9b) show that the time evolution of $\mathbf{p}_\pm$ only arises from the evolution of the constant t hypersurfaces at the infinities. Thus, in this local canonical chart on $\tilde{\Gamma}_\eta$, the information about the shell motion is encoded in equations (4.9b).

It should be emphasized that the degrees of freedom present in $\mathbf{p}_\pm$ are invariant under the isometries of the spacetime. Killing time translations on the spacetime move both the shell history and the constant t hypersurface: in particular, they move the two asymptotic ends of the constant t hypersurface, and hence the asymptotic ends of the associated asymptotically null hypersurface. However, the Eddington-Finkelstein time *differences* that constitute the momenta are invariant under Killing time translations.

As we have assumed that the shell history does not lie on a horizon, the coordinates $(\mathbf{m}_+,\mathbf{m}_-,\mathbf{p}_+,\mathbf{p}_-)$ do not form a global chart on $\tilde{\Gamma}_\eta$. Instead, these coordinates provide two disjoint local canonical charts, covering two disconnected sets in $\tilde{\Gamma}_\eta$: one for $0<\mathbf{m}_-<\mathbf{m}_+$ and the other for $0<\mathbf{m}_+<\mathbf{m}_-$, with unrestricted values of $\mathbf{p}_\pm$ in each chart. These coordinates cannot be extended to $\mathbf{m}_+=\mathbf{m}_-$. The reason is that when $\mathbf{m}_+=\mathbf{m}_-$, the shell history lies on a horizon, the singularity in Π_M is at $r=\mathfrak{r}$, and the first term under each integral in (4.7) makes both $\mathbf{p}_+$ and $\mathbf{p}_-$ divergent. We shall address the special case $\mathbf{m}_+=\mathbf{m}_-$ and the global structure of $\tilde{\Gamma}_\eta$ in subsection IV B.

It will be useful to introduce on $\tilde{\Gamma}_\eta$ another set of local canonical coordinates, $(\overline{\mathbf{m}},\tilde{\mathbf{m}},\overline{\mathbf{p}},\tilde{\mathbf{p}})$, by the transformation

$$\overline{\mathbf{m}}=\tfrac{1}{2}(\mathbf{m}_++\mathbf{m}_-), \tag{4.10a}$$

$$\tilde{\mathbf{m}}=\tfrac{1}{2}(\mathbf{m}_+-\mathbf{m}_-), \tag{4.10b}$$

$$\overline{\mathbf{p}}=\mathbf{p}_++\mathbf{p}_-, \tag{4.10c}$$

$$\tilde{\mathbf{p}}=\mathbf{p}_+-\mathbf{p}_-. \tag{4.10d}$$

The inverse transformation is

$$\mathbf{m}_\pm=\overline{\mathbf{m}}\pm\tilde{\mathbf{m}}, \tag{4.11a}$$

$$\mathbf{p}_\pm=\tfrac{1}{2}(\overline{\mathbf{p}}\pm\tilde{\mathbf{p}}). \tag{4.11b}$$

From (4.7), (4.10c), and (4.10d), we see that $\overline{\mathbf{p}}$ contains the information about the asymptotic ends of the constant t hypersurface, whereas the information about the location of the shell with respect to the infinities is encoded in $\tilde{\mathbf{p}}$. We can therefore loosely regard the pair $(\overline{\mathbf{m}},\overline{\mathbf{p}})$ as describing the vacuum spacetime dynamics, and the pair $(\tilde{\mathbf{m}},\tilde{\mathbf{p}})$ as describing the shell. While not literal, this view will be helpful for understanding the global structure of $\tilde{\Gamma}_\eta$ in subsections IV B and IV C.

As defined by the transformation (4.10), the coordinates $(\overline{\mathbf{m}},\tilde{\mathbf{m}},\overline{\mathbf{p}},\tilde{\mathbf{p}})$ provide two disjoint local canonical charts that cover on $\tilde{\Gamma}_\eta$ the same two disconnected sets as the coordinates $(\mathbf{m}_+,\mathbf{m}_-,\mathbf{p}_+,\mathbf{p}_-)$. The ranges of the variables in these two charts are respectively $0<\tilde{\mathbf{m}}<\overline{\mathbf{m}}$ and $0<-\tilde{\mathbf{m}}<\overline{\mathbf{m}}$, each with unrestricted $\overline{\mathbf{p}}$ and $\tilde{\mathbf{p}}$. The coordinates $(\overline{\mathbf{m}},\tilde{\mathbf{m}},\overline{\mathbf{p}},\tilde{\mathbf{p}})$ cannot, however, be extended to $\tilde{\mathbf{m}}=0$. While $\overline{\mathbf{p}}$ remains finite for a horizon-straddling shell, it is seen from (4.7) that $\tilde{\mathbf{p}}$ must diverge.

B. Shell on a horizon

We now wish to find on $\tilde{\Gamma}_\eta$ coordinates that extend to the horizon-straddling shell. We shall first rely on the spacetime picture to identify the geometrical information that the coordinates must carry in this limit. We then construct on $\tilde{\Gamma}_\eta$ a global canonical chart that contains this information.

Consider the spacetime of Fig. 1. The shell is left-moving, corresponding to $\eta=-1$, and the shell history lies in the future of the left-going horizon, corresponding to $\mathbf{m}_+>\mathbf{m}_-$. The points A and B indicate the ends of the asymptotically null hypersurface that is associated to the hypersurface of constant t. $\mathbf{p}_+$ is the difference in the Eddington-Finkelstein time between points p_1 and q_1, and $\mathbf{p}_-$ is the difference in the Eddington-Finkelstein time between points q_2 and p_2.

In this spacetime, let γ_1 be the radial null geodesic connecting p_1 to q_1, let γ_2 the radial null geodesic connecting q_2 to p_2, and let γ_3 be the radial null geodesic connecting p_1 to p_2. Let λ_i $(i=1,2,3)$ be the affine parameters on these geodesics, each normalized to have the range $[0,1]$. λ_2 and λ_3 increase toward the future. λ_1 increases toward the future if q_1 is in the future of p_1 as shown in the figure, corresponding to $\mathbf{p}_+<0$, and it increases towards the past if q_1 is in the past of p_1, corresponding to $\mathbf{p}_+>0$. In the special case $\mathbf{p}_+=0$, q_1 and p_1 coincide, and γ_1 degenerates to a point. We now define the quantities $Q_\pm$ by

$$Q_+:=(\partial/\partial\lambda_1)_a(\partial/\partial\lambda_3)^a\big|_{p_1}, \tag{4.12a}$$

$$Q_-:=(\partial/\partial\lambda_2)_a(\partial/\partial\lambda_3)^a\big|_{p_2}. \tag{4.12b}$$

Similarly, consider a spacetime in which $\eta=-1$ but the shell history lies in the past of the left-going horizon, corre-

sponding to $\mathbf{m}_+<\mathbf{m}_-$. In this spacetime, the counterparts of points p_1 and p_2 are below the left-going horizon, but the three null geodesics γ_i ($i=1,2,3$) can be defined as above, the only modification being that the potentially degenerate one is now γ_2. In this spacetime, we again define $Q_\pm$ by (4.12).

A straightforward calculation yields

$$Q_+ = -8\mathbf{m}_+\left[\mathbf{m}_- - \mathbf{m}_+ + |\mathbf{m}_+ - \mathbf{m}_-|\exp\left(-\frac{\mathbf{p}_+}{4\mathbf{m}_+}\right)\right], \tag{4.13a}$$

$$Q_- = -8\mathbf{m}_-\left[\mathbf{m}_+ - \mathbf{m}_- + |\mathbf{m}_+ - \mathbf{m}_-|\exp\left(\frac{\mathbf{p}_-}{4\mathbf{m}_-}\right)\right], \tag{4.13b}$$

valid both for $\mathbf{m}_+>\mathbf{m}_-$ and $\mathbf{m}_+<\mathbf{m}_-$. The canonical coordinates $(\mathbf{m}_+,\mathbf{m}_-,\mathbf{p}_+,\mathbf{p}_-)$ can therefore be replaced by the noncanonical coordinates $(\mathbf{m}_+,\mathbf{m}_-,Q_+,Q_-)$, with $Q_-<0$ for $\mathbf{m}_+>\mathbf{m}_-$ and $Q_+<0$ for $\mathbf{m}_+<\mathbf{m}_-$.

The crucial observation is now that $Q_\pm$, as defined in (4.12), remain well defined also for the spacetimes shown in Fig. 2, in which $\mathbf{m}_+=\mathbf{m}_-$ and the shell history lies on a common horizon. In these spacetimes, $Q_\pm$ can each take arbitrary negative values. As the soldering along the horizon is affine, $Q_\pm$ precisely encode the coordinate-invariant information about the relative loci of the points p_1, p_2, A, and B (or, equivalently, the points p_1, p_2, q_1, and q_2). This means that the set $(\mathbf{m}_+,\mathbf{m}_-,Q_+,Q_-)$ provides a global, noncanonical chart on $\widetilde{\Gamma}_-$. The domain is $Q_-<0$ for $\mathbf{m}_+>\mathbf{m}_-$, $Q_+<0$ for $\mathbf{m}_+<\mathbf{m}_-$, and $Q_\pm<0$ for $\mathbf{m}_+=\mathbf{m}_-$.

In the above construction we have taken $\eta=-1$. It is clear that an entirely analogous discussion carries through for $\eta=1$, with straightforward changes in formulas (4.13), and yielding a global, noncanonical chart on on $\widetilde{\Gamma}_+$.

To find a global *canonical* chart on $\widetilde{\Gamma}_\eta$, consider the transformation

$$\overline{\boldsymbol{\pi}} := \overline{\mathbf{p}} + 8\eta\widetilde{\mathbf{m}}(\ln|\widetilde{\mathbf{m}}/\overline{\mathbf{m}}|-1), \tag{4.14a}$$

$$\widetilde{\boldsymbol{\pi}} := \widetilde{\mathbf{p}} + 8\eta\overline{\mathbf{m}}(\ln|\widetilde{\mathbf{m}}/\overline{\mathbf{m}}|+1). \tag{4.14b}$$

Equations (4.14) clearly define a canonical transformation from $(\overline{\mathbf{m}},\widetilde{\mathbf{m}},\overline{\mathbf{p}},\widetilde{\mathbf{p}})$ to $(\overline{\mathbf{m}},\widetilde{\mathbf{m}},\overline{\boldsymbol{\pi}},\widetilde{\boldsymbol{\pi}})$ individually in the domains $0<\widetilde{\mathbf{m}}<\overline{\mathbf{m}}$ and $0<-\widetilde{\mathbf{m}}<\overline{\mathbf{m}}$. It is straightforward to verify that the chart $(\overline{\mathbf{m}},\widetilde{\mathbf{m}},\overline{\boldsymbol{\pi}},\widetilde{\boldsymbol{\pi}})$ becomes global on $\widetilde{\Gamma}_\eta$ when extended to $\widetilde{\mathbf{m}}=0$ with unrestricted values of $\overline{\boldsymbol{\pi}}$ and $\widetilde{\boldsymbol{\pi}}$. For $\eta=-1$, in particular, (4.13) shows that $Q_\pm$ can be written as

$$Q_+ = -16(\overline{\mathbf{m}}+\widetilde{\mathbf{m}})\left\{\overline{\mathbf{m}}\exp\left[-\left(\frac{\overline{\mathbf{m}}-\widetilde{\mathbf{m}}}{\overline{\mathbf{m}}+\widetilde{\mathbf{m}}}\right)-\frac{\overline{\boldsymbol{\pi}}+\widetilde{\boldsymbol{\pi}}}{8(\overline{\mathbf{m}}+\widetilde{\mathbf{m}})}\right]-\widetilde{\mathbf{m}}\right\}, \tag{4.15a}$$

$$Q_- = -16(\overline{\mathbf{m}}-\widetilde{\mathbf{m}})\left\{\overline{\mathbf{m}}\exp\left[-\left(\frac{\overline{\mathbf{m}}+\widetilde{\mathbf{m}}}{\overline{\mathbf{m}}-\widetilde{\mathbf{m}}}\right)+\frac{\overline{\boldsymbol{\pi}}-\widetilde{\boldsymbol{\pi}}}{8(\overline{\mathbf{m}}-\widetilde{\mathbf{m}})}\right]+\widetilde{\mathbf{m}}\right\}, \tag{4.15b}$$

from which the regularity of the $\widetilde{\mathbf{m}}\to 0$ limit is manifest.

We have thus shown that the set $(\overline{\mathbf{m}},\widetilde{\mathbf{m}},\overline{\boldsymbol{\pi}},\widetilde{\boldsymbol{\pi}})$ provides a global canonical chart on $\widetilde{\Gamma}_\eta$. The domain of the variables is $|\widetilde{\mathbf{m}}|<\overline{\mathbf{m}}$, with $\overline{\boldsymbol{\pi}}$ and $\widetilde{\boldsymbol{\pi}}$ taking all real values. We therefore have $\widetilde{\Gamma}_\eta\simeq\mathbb{R}^4$. The Hamiltonian reads

$$\mathbf{h}=(N_++N_-)\overline{\mathbf{m}}+(N_+-N_-)\widetilde{\mathbf{m}}. \tag{4.16}$$

The values of $\overline{\mathbf{m}}$ and $\widetilde{\mathbf{m}}$ are constants of motion, whereas the equations of motion for $\overline{\boldsymbol{\pi}}$ and $\widetilde{\boldsymbol{\pi}}$ show that the evolution of $Q_\pm$ only arises from the evolution of the constant t hypersurface at the two spacelike infinities. This means that the information about the shell dynamics is contained in the momentum equations of motion both for $\widetilde{\mathbf{m}}\neq 0$ (as was already seen in subsection IV A) as well as for $\widetilde{\mathbf{m}}=0$.

C. Test shell limit

We have so far assumed that the unreduced shell momentum $\mathfrak{p}$ is nonvanishing. We saw that this assumption is compatible with the dynamics, and that it divides the reduced phase space into the two disconnected sectors $\widetilde{\Gamma}_\eta$, labeled by $\eta=\mathrm{sign}(\mathfrak{p})$. As the unreduced bulk action (2.6) is not differentiable in $\mathfrak{p}$ at $\mathfrak{p}=0$, it is not clear whether $\widetilde{\Gamma}_+$ and $\widetilde{\Gamma}_-$ are joinable to each other in any smooth sense. Our reduction formalism is not well suited to examining this issue: the canonical transformation of Sec. III was tailored to the null hypersurfaces separately for $\eta=\pm 1$.

We can, however, address the limit $\mathfrak{p}\to 0$ *individually* in $\widetilde{\Gamma}_+$ and $\widetilde{\Gamma}_-$. As the shell stress-energy tensor (2.11) vanishes for $\mathfrak{p}\to 0$, this is the limit of a test shell that traverses the spacetime without affecting it gravitationally. We shall now show that one can attach the right-moving and left-moving test shell limits respectively to $\widetilde{\Gamma}_+$ and $\widetilde{\Gamma}_-$ as smooth boundaries with topology $\mathbb{R}^3$.

When the test shell history does not lie on a horizon, the situation is straightforward. We can start with the coordinates $(\mathbf{m}_+,\mathbf{m}_-,\mathbf{p}_+,\mathbf{p}_-)$, separately for $0<\mathbf{m}_-<\mathbf{m}_+$ and $0<\mathbf{m}_+<\mathbf{m}_-$, and simply take the limit $\mathbf{m}_+=\mathbf{m}_-$ with $\mathbf{p}_\pm$ remaining finite. From the geometrical interpretation of $\mathbf{p}_\pm$ it is seen that this attaches to $\widetilde{\Gamma}_\eta$ those test shell configurations in which the test shell does not straddle a horizon. The locus of the test shell history is determined by $\mathbf{p}_\pm$ exactly as in subsection IV A.

Including a horizon-straddling test shell is more intricate. In the global chart $(\overline{\mathbf{m}},\widetilde{\mathbf{m}},\overline{\boldsymbol{\pi}},\widetilde{\boldsymbol{\pi}})$, the limit of a test shell on a horizon is achieved by setting first $\widetilde{\mathbf{m}}=0$ and then taking $\eta\widetilde{\boldsymbol{\pi}}\to-\infty$ while keeping $\overline{\boldsymbol{\pi}}$ finite. On the other hand, the limit of a test shell off the horizon requires taking simultaneously $\widetilde{\mathbf{m}}\to 0$ and $\eta\widetilde{\boldsymbol{\pi}}\to-\infty$ so that $\overline{\mathbf{p}}$ and $\widetilde{\mathbf{p}}$ remain finite. What we need is a new canonical chart in which both of these limits are brought to finite values of the coordinates.

To this end, let

$$x := \exp\left(\frac{\eta\widetilde{\boldsymbol{\pi}}}{8\overline{\mathbf{m}}}\right), \tag{4.17a}$$

$$p_x := -8\,\eta\tilde{\mathbf{m}}\bar{\mathbf{m}}\exp\left(-\frac{\eta\tilde{\boldsymbol{\pi}}}{8\bar{\mathbf{m}}}\right), \tag{4.17b}$$

$$\bar{\mathbf{\Pi}} := \bar{\boldsymbol{\pi}} - \frac{\tilde{\boldsymbol{\pi}}\tilde{\mathbf{m}}}{\bar{\mathbf{m}}}. \tag{4.17c}$$

As

$$\bar{\mathbf{\Pi}}\delta\bar{\mathbf{m}} + p_x\delta x = \bar{\boldsymbol{\pi}}\delta\bar{\mathbf{m}} + \tilde{\boldsymbol{\pi}}\delta\tilde{\mathbf{m}} - \delta(\tilde{\boldsymbol{\pi}}\tilde{\mathbf{m}}), \tag{4.18}$$

equations (4.17) define a canonical transformation from the chart $(\bar{\mathbf{m}},\tilde{\mathbf{m}},\bar{\boldsymbol{\pi}},\tilde{\boldsymbol{\pi}})$ to the chart $(\bar{\mathbf{m}},x,\bar{\mathbf{\Pi}},p_x)$. The new canonical chart is global: the range is $\bar{\mathbf{m}}>0$ and $x>0$, with unrestricted $\bar{\mathbf{\Pi}}$ and p_x. The qualitative location of the shell history is governed by the sign of p_x: $p_x>0$ ($p_x<0$) yields a shell in the future (past) of the horizon that is parallel to the shell history, while $p_x=0$ yields a shell history on the horizon. It is now easily seen that in this chart the test shell limit is $x\to 0$, with the other coordinates remaining at finite values. A horizon-straddling test shell is recovered with $p_x=0$, whereas $p_x>0$ ($p_x<0$) gives a test shell in the future (past) of the horizon that the test shell does not cross. Clearly, the test shell limit constitutes a smooth boundary of $\tilde{\Gamma}_\eta$ with topology $\mathbb{R}^3$.

V. HAMILTONIAN FOR THE SHELL RADIUS IN STATIONARY EXTERIOR COORDINATES

While the charts on $\tilde{\Gamma}_\eta$ introduced in Sec. IV are well adapted to the geometry of the spacetime, they contain the information about the shell motion in a nontransparent manner. In this section we introduce on $\tilde{\Gamma}_\eta$ a local canonical chart that describes more directly the motion of the shell in the spacetime geometry. A chart of this kind is of particular physical interest if one wishes to quantize the system as a model of black hole radiation with back reaction [30,31,34].

The physical situation we have in mind is a static observer who scrutinizes the shell motion from an asymptotically flat infinity. For definiteness, we take this infinity to be the right-hand-side one. We set $N_+=1$, so that the coordinate time t coincides with the observer's proper time. To incorporate the observer's ignorance of what is happening at the left-hand-side infinity, we set $N_-=0$.

We further assume that the shell history reaches a future or past null infinity on the right-hand side. The Penrose diagram for $\eta=-1$ is therefore as in Fig. 1, and the Penrose diagram for $\eta=1$ is the time inverse. In particular, we have $\mathbf{m}_-<\mathbf{m}_+$, and we are in the region of $\tilde{\Gamma}_\eta$ covered by the chart $(\mathbf{m}_+,\mathbf{m}_-,\mathbf{p}_+,\mathbf{p}_-)$ with $0<\mathbf{m}_-<\mathbf{m}_+$.

Consider thus the chart $(\mathbf{m}_+,\mathbf{m}_-,\mathbf{p}_+,\mathbf{p}_-)$ with $0<\mathbf{m}_-<\mathbf{m}_+$. From Sec. IV we recall that the pair $(\mathbf{m}_+,\mathbf{p}_+)$ only carries information about the geometry right of the shell, and the pair $(\mathbf{m}_-,\mathbf{p}_-)$ only carries information about the geometry left of the shell. To describe the motion of the shell as seen from the right-hand-side infinity, we can therefore leave the pair $(\mathbf{m}_-,\mathbf{p}_-)$ intact and seek a canonical transformation that replaces $(\mathbf{m}_+,\mathbf{p}_+)$ by a new pair.

To specify the new pair, we choose in the Kruskal geometry right of the shell a stationary coordinate system that conforms to the falloff (2.12) with $N_+=1$. As $R(r)$ is then an increasing function, we can assume $R(r)=r$ without loss of generality. Let $\hat{r}$ stand for the shell curvature radius in these coordinates: $\hat{r}(t):=R(\mathfrak{r}(t))=\mathfrak{r}(t)$. We now seek a momentum $\hat{p}$ such that there is a canonical transformation from the pair $(\mathbf{m}_+,\mathbf{p}_+)$ to the pair $(\hat{r},\hat{p})$. Writing the transformation as $\mathbf{p}_+=\mathbf{p}_+(\hat{r},\mathbf{m}_+)$ and $\hat{p}=\hat{p}(\hat{r},\mathbf{m}_+)$, the canonicality criterion reads

$$\frac{\partial[\hat{p}(\hat{r},\mathbf{m}_+)]}{\partial\mathbf{m}_+} = -\frac{\partial[\mathbf{p}_+(\hat{r},\mathbf{m}_+)]}{\partial\hat{r}}. \tag{5.1}$$

Substituting $\mathbf{p}_+$ from (4.7a) to the right-hand side of (5.1) yields

$$\frac{\partial[\hat{p}(\hat{r},\mathbf{m}_+)]}{\partial\mathbf{m}_+} = \Pi_M(\hat{r},\mathbf{m}_+), \tag{5.2}$$

where $\Pi_M(r,\mathbf{m}_+)$ is determined by the choice of the stationary coordinate system. Note that the convergence functions $G(r)$ and $g_+(r)$ have not entered (5.2). Solving the differential equation (5.2) for $\hat{p}(\hat{r},\mathbf{m}_+)$ yields the desired canonical transformation, and inverting this solution gives $\mathbf{m}_+(\hat{r},\hat{p})$ as a function in the new canonical chart. The action reads

$$S=\int dt[\mathbf{p}_-\dot{\mathbf{m}}_- + \hat{p}\dot{\hat{r}} - \mathbf{m}_+(\hat{r},\hat{p})]. \tag{5.3}$$

The shell stress-energy tensor in the new chart can be found using (2.10), (2.11) and (4.5).

As explicit examples, we now present the shell Hamiltonians $\mathbf{m}_+(\hat{r},\hat{p})$ in four different stationary coordinate systems. We arrived at the first three coordinate systems by seeking a simple functional form for $\mathbf{m}_+(\hat{r},\hat{p})$. The fourth coordinate system is the spatially flat one used in Ref. [30].

A. Polynomial gauge

As a first example, we consider coordinates in which the metric reads

$$R=r, \tag{5.4a}$$

$$\Lambda^2=N^{-2}=1+2\mathbf{m}_+/r+(2\mathbf{m}_+/r)^2+(2\mathbf{m}_+/r)^3, \tag{5.4b}$$

$$\Lambda^2 N^r = -\eta(2\mathbf{m}_+/r)^2. \tag{5.4c}$$

With $r>0$, these coordinates cover half of Kruskal manifold in the appropriate manner, and the falloff (2.12) is satisfied with $\epsilon=1$. The relation to the curvature coordinates is

$$R=r, \tag{5.5a}$$

$$T=t+2\,\eta\mathbf{m}_+\,\ln|1-2\mathbf{m}_+/r|. \tag{5.5b}$$

We find

$$\Pi_M(r,\mathbf{m}_+)=\eta(1+2\mathbf{m}_+/r). \tag{5.6}$$

Solving (5.2) with a convenient choice for the integration constant, we obtain

$$\mathbf{m}_+(\hat{r},\hat{p})=\sqrt{\eta\hat{p}\hat{r}}-\tfrac{1}{2}\hat{r}. \tag{5.7}$$

The equation of motion derived from the Hamiltonian (5.7) can be integrated as $\eta t=\hat{r}+2\mathbf{m}_+\ \ln(\hat{r}/\mathbf{m}_+)+\text{constant}$. It is easily verified that this is the correct equation for a null geodesic in the metric (5.4).

B. Exponential gauge

Consider next coordinates in which the metric reads

$$R=r, \tag{5.8a}$$

$$\Lambda^2=N^{-2}=\exp(2\mathbf{m}_+/r)[2-(1-2\mathbf{m}_+/r)\exp(2\mathbf{m}_+/r)], \tag{5.8b}$$

$$\Lambda^2N^r=-\eta[1-(1-2\mathbf{m}_+/r)\exp(2\mathbf{m}_+/r)]. \tag{5.8c}$$

With $r>0$, these coordinates cover half of Kruskal manifold in the appropriate manner, and the falloff (2.12) is satisfied with $\epsilon=1$. The relation to the curvature coordinates is

$$R=r, \tag{5.9a}$$

$$T=t+\eta\int^r[(1-2\mathbf{m}_+/r')^{-1}-\exp(2\mathbf{m}_+/r')]dr'. \tag{5.9b}$$

We find

$$\Pi_M(r,\mathbf{m}_+)=\eta\ \exp(2\mathbf{m}_+/r). \tag{5.10}$$

Solving (5.2) with a convenient choice for the integration constant, we obtain

$$\mathbf{m}_+(\hat{r},\hat{p})=\tfrac{1}{2}\hat{r}\ \ln(2\eta\hat{p}/\hat{r}). \tag{5.11}$$

The equation of motion can be solved implicitly in terms of the exponential integral function.

C. Eddington-Finkelstein–type gauge

Consider next coordinates in which the metric reads

$$R=r, \tag{5.12a}$$

$$\Lambda^2=N^{-2}=1+2\mathbf{m}_+/r, \tag{5.12b}$$

$$\Lambda^2N^r=-2\eta\mathbf{m}_+/r. \tag{5.12c}$$

With $r>0$, these coordinates cover half of Kruskal manifold in the appropriate manner. The relation to the curvature coordinates is

$$R=r, \tag{5.13a}$$

$$T=t+2\eta\mathbf{m}_+\ln|r/(2\mathbf{m}_+)-1|. \tag{5.13b}$$

We recognize these coordinates as simply related to the Eddington-Finkelstein coordinates [47]: $t-\eta r$ is the retarded (advanced) Eddington-Finkelstein time for $\eta=1$ ($\eta=-1$). In terms of the tortoise coordinate $r^*:=r+2\mathbf{m}_+\ln[r/(2\mathbf{m}_+)-1]$, we have $t-\eta r=T-\eta r^*$.

There is a minor technical issue in that the coordinates (5.12) do not obey the falloff (2.12): we have $P_\Lambda=-2\eta\mathbf{m}_+(1+2\mathbf{m}_+/r)^{-1/2}$, which violates (2.12c). We therefore take the coordinates (5.12) to hold for $r<R_{\rm cut}$, where $R_{\rm cut}$ is a large parameter, and smoothly deform them to a faster falloff for $r>R_{\rm cut}$. As equation (5.2) is local in $\hat{r}$, the form of the canonical transformation for $r<R_{\rm cut}$ is independent of that for $r>R_{\rm cut}$. In the end, we can either leave the Hamiltonian unspecified for $r>R_{\rm cut}$, or argue that one can take the limit $R_{\rm cut}\to\infty$ in the sense of some suitable renormalization in the parameters of the canonical transformation.

Proceeding in this way, we find

$$\Pi_M(r,\mathbf{m}_+)=\eta, \tag{5.14}$$

and, with a convenient choice of the integration constant,

$$\mathbf{m}_+(\hat{r},\hat{p})=\eta\hat{p}. \tag{5.15}$$

The Hamiltonian (5.15) clearly correctly reproduces the fact that the Eddington-Finkelstein time $t-\eta r$ is constant on the shell history.

D. Spatially flat gauge

As the last example, we consider coordinates in which the metric reads

$$R=r, \tag{5.16a}$$

$$\Lambda=N=1, \tag{5.16b}$$

$$N^r=-\eta\sqrt{2\mathbf{m}_+/r}. \tag{5.16c}$$

With $r>0$, these coordinates cover half of Kruskal manifold in the appropriate manner. The relation to the curvature coordinates is

$$R=r, \tag{5.17a}$$

$$T=t+2\eta\left(\sqrt{2\mathbf{m}_+r}+\mathbf{m}_+\ln\left|\frac{1-\sqrt{2\mathbf{m}_+/r}}{1+\sqrt{2\mathbf{m}_+/r}}\right|\right). \tag{5.17b}$$

We recognize these coordinates as the spatially flat coordinates [43–45], recently employed in the study of Hawking radiation with back reaction in Ref. [30].

There is again a minor technical issue in that the coordinates (5.16) do not obey the falloff (2.12). A Hamiltonian falloff analysis compatible with these coordinates has been discussed in the metric variables in Ref. [37]. Here, however, we shall simply argue in terms of a cutoff parameter $R_{\rm cut}$ as above. We have

$$\Pi_M(r,\mathbf{m}_+)=\frac{\eta}{1+\sqrt{2\mathbf{m}_+/r}}, \tag{5.18}$$

and solving (5.2) with a suitable integration constant yields $\mathbf{m}_+(\hat{r},\hat{p})$ implicitly as the solution to

$$\eta\hat{p}=\sqrt{2\mathbf{m}_+\hat{r}}-\hat{r}\,\ln(1+\sqrt{2\mathbf{m}_+/\hat{r}}). \tag{5.19}$$

In order to make a connection to the work in Ref. [30], we define

$$p_c:=\hat{p}-\eta[\sqrt{2\mathbf{m}_-\hat{r}}-\hat{r}\,\ln(1+\sqrt{2\mathbf{m}_-/\hat{r}})], \tag{5.20a}$$

$$\mathbf{p}_c:=\mathbf{p}_--\eta[\hat{r}-2\sqrt{2\mathbf{m}_-\hat{r}}+4\mathbf{m}_-\ln(1+\sqrt{\hat{r}/(2\mathbf{m}_-)})]. \tag{5.20b}$$

Equations (5.20) define a canonical transformation from the chart $(\hat{r},\mathbf{m}_-,\hat{p},\mathbf{p}_-)$ to the new canonical chart $(\hat{r},\mathbf{m}_-,p_c,\mathbf{p}_c)$. The Hamiltonian $\mathbf{m}_+(\hat{r},\mathbf{m}_-,p_c)$ in the new chart is obtained (in implicit form) by eliminating $\hat{p}$ from (5.19) and (5.20a). As the value of $\mathbf{m}_-$ is a constant of motion, the system can be partially reduced by regarding $\mathbf{m}_-$ as a prescribed constant. The term $\int dt\mathbf{p}_c\dot{\mathbf{m}}_-$ then drops from the action, and we obtain

$$S=\int dt[p_c\dot{\hat{r}}-\mathbf{m}_+(\hat{r},\mathbf{m}_-,p_c)]. \tag{5.21}$$

For $\eta=-1$, this is the action derived in Refs. [30, 37] by different methods. For $\eta=1$, it is not. The reason is that the coordinates (5.16) are the ingoing spatially flat coordinates for $\eta=-1$ and the outgoing spatially flat coordinates for $\eta=1$, thus covering all of the spacetime right of the shell in each case, whereas Ref. [30] was physically motivated to use the ingoing spatially flat coordinates irrespectively the direction of the shell motion. It would be straightforward to repeat the above analysis with the sign of η in (5.16) reversed, recovering the result of Refs. [30, 37] for $\eta=1$. Note, however, that with the sign of η in (5.16) reversed, the coordinates do not cover the part of the shell history that lies inside the horizon.

VI. PARAMETRIZATION CLOCKS AT THE INFINITIES

In the previous sections we fixed the evolution of the spatial hypersurfaces at the spacelike infinities by taking $N_\pm$ to be prescribed functions of t. In this section we free this evolution by making the replacement [10]

$$N_\pm=\pm\dot{\tau}_\pm \tag{6.1}$$

in the boundary term in the actions (2.13) and (3.21). The variations of N become then unrestricted at $r\to\pm\infty$, but varying the action with respect to $\tau_\pm$ yields the relations (6.1) as equations of motion. The new variables $\tau_\pm$ are the proper times measured by static standard clocks at the respective infinities, with the convention that τ_+ increases toward the future and τ_- increases toward the past.

In the absence of a shell, it was shown in Ref. [10] that the action containing $\tau_\pm$ as independent variables can be brought to a canonical form in which the unconstrained degrees of freedom and the pure gauge degrees of freedom are entirely decoupled. We now outline the analogous result in the presence of the null shell. For brevity, we shall refrain from explicitly spelling out the smoothness properties of the various emerging phase space functions.

We start from the action (3.21), with g given by (4.1), and we make in the boundary term the replacement (6.1). The resulting action is a sum of two decoupled parts: a Hamiltonian action S_{R} consisting of the terms that contain the pair $(\mathsf{R},\Pi_{\mathsf{R}})$, and the remainder S_0. We only need to consider S_0. As in Sec. III, we assume first that the shell history does not lie on a horizon, and relax this assumption at the end.

Under the time integral in S_0, the terms homogeneous in the time derivatives are

$$\Theta:=\mathfrak{p}\dot{\mathfrak{r}}-M_+\dot{\tau}_++M_-\dot{\tau}_-+\int_{-\infty}^{\infty}dr[(\Pi_M-\eta G)\dot{M}-\eta\dot{g}]. \tag{6.2}$$

We pass from the noncanonical chart $(\mathfrak{r},M(r),\mathfrak{p},\Pi_M(r);\tau_+,\tau_-)$ to the new chart $(\overline{m},\mathfrak{r},\Gamma(r),\overline{p},\mathfrak{p},\Pi_\Gamma(r))$, defined by

$$\Gamma(r):=M'(r), \tag{6.3a}$$

$$\Pi_\Gamma(r)=\tfrac{1}{2}(\tau_++\tau_-)+\int_{-\infty}^{\infty}dr'\{\tfrac{1}{2}[\Pi_M(r')-\eta G(r')]\times[\theta(r'-r)-\theta(r-r')]-\eta M_+g_+(r')+\eta M_-g_-(r')\}, \tag{6.3b}$$

$$\overline{m}:=\tfrac{1}{2}(M_++M_-), \tag{6.3c}$$

$$\overline{p}:=\tau_+-\tau_-+\int_{-\infty}^{\infty}dr\{[\Pi_M(r)-\eta G(r)]-2\eta M_+g_+(r)-2\eta M_-g_-(r)\}. \tag{6.3d}$$

The falloff is

$$\Gamma(t,r)=O^\infty(|r|^{-1-\epsilon}), \tag{6.4a}$$

$$\Pi_\Gamma(t,r)=-2\eta M_\pm\ln|r/M_\pm|+O^\infty(|r|^0). \tag{6.4b}$$

By techniques similar to those in Ref. [10], we find

$$\Theta=\mathfrak{p}\dot{\mathfrak{r}}+\overline{p}\dot{\overline{m}}+\int_{-\infty}^{\infty}dr\Pi_\Gamma(r)\dot{\Gamma}(r)+\frac{d}{dt}(M_+\tau_++M_-\tau_-). \tag{6.5}$$

The chart $(\overline{m},\mathfrak{r},\Gamma(r),\overline{p},\mathfrak{p},\Pi_\Gamma(r))$ is therefore canonical. Dropping the integral of a total derivative, the action reads

$$S_0=\int dt\left(\mathfrak{p}\dot{\mathfrak{r}}+\overline{p}\dot{\overline{m}}+\int_{-\infty}^{\infty}dr\Pi_\Gamma\dot{\Gamma}\right)-\int dt\int_{-\infty}^{\infty}dr\widetilde{N}[\Gamma-\mathfrak{p}(\eta G-\Pi_\Gamma')^{-1}\times\delta(r-\mathfrak{r})]. \tag{6.6}$$

To express the constraint in the new chart, we have used equation (6.3a) and the relation $\Pi_M=\eta G-\Pi_\Gamma'$, which follows by differentiating (6.3b).

The action (6.6) is canonical, but the constraint couples the variables in a nontransparent way. To decouple the degrees of freedom, we pass to the chart $(\overline{m},\widetilde{m},\widetilde{\Gamma}(r),\overline{p},\widetilde{p},\Pi_{\widetilde{\Gamma}}(r))$, defined by

$$\widetilde{\Gamma}(r):=\Gamma(r)-\mathfrak{p}[\,\eta G(r)-\Pi_\Gamma'(r)\,]^{-1}\delta(r-\mathfrak{r}), \quad (6.7a)$$

$$\Pi_{\widetilde{\Gamma}}(r):=\Pi_\Gamma(r), \quad (6.7b)$$

$$\widetilde{m}:=\tfrac{1}{2}\mathfrak{p}(\,\eta\hat{G}-\widehat{\Pi_\Gamma'})^{-1}, \quad (6.7c)$$

$$\widetilde{p}:=2\widehat{\Pi_\Gamma}-2\,\eta\int_0^{\mathfrak{r}}dr\,G(r). \quad (6.7d)$$

The falloff of $\widetilde{\Gamma}$ and $\Pi_{\widetilde{\Gamma}}$ is clearly the same as that of Γ and Π_Γ, given in (6.4). Using the analogue of relation (A4) for Π_Γ, we find

$$\dot{\mathfrak{p}}\mathfrak{r}-\widetilde{p}\dot{\widetilde{m}}+\int_{-\infty}^{\infty}dr(\Pi_\Gamma\dot{\Gamma}-\Pi_{\widetilde{\Gamma}}\dot{\widetilde{\Gamma}})=\frac{d}{dt}\left[2\,\eta\widetilde{m}\int_0^{\mathfrak{r}}dr\,G(r)\right]. \quad (6.8)$$

The chart $(\overline{m},\widetilde{m},\widetilde{\Gamma}(r),\overline{p},\widetilde{p},\Pi_{\widetilde{\Gamma}}(r))$ is therefore canonical. Dropping the integral of a total derivative, the action reads

$$S_0=\int dt\left(\overline{p\dot{m}}+\widetilde{p}\dot{\widetilde{m}}+\int_{-\infty}^{\infty}dr\,\Pi_{\widetilde{\Gamma}}\dot{\widetilde{\Gamma}}\right)-\int dt\int_{-\infty}^{\infty}dr\widetilde{N}\widetilde{\Gamma}. \quad (6.9)$$

The unconstrained canonical degrees of freedom, $(\overline{m},\widetilde{m},\overline{p},\widetilde{p})$, have now become decoupled from the pure gauge degrees of freedom.

To put the action in a more transparent form, we write

$$V(r):=\Pi_{\widetilde{\Gamma}}(r)+\tfrac{1}{2}\overline{p}-\eta\int_0^r dr'\,G(r')$$

$$=\tau_+ +\int_{-\infty}^{\infty}dr'[\,\Pi_M(r')\,\theta(r'-r)-\eta G(r')\,\theta(r')$$

$$-2\,\eta M_+ g_+(r')], \quad (6.10a)$$

$$\Pi_V(r):=-\widetilde{\Gamma}(r). \quad (6.10b)$$

The falloff is

$$V(t,r)=-\,\eta|r|-2\,\eta M_\pm\ln|r/M_\pm|+O^\infty(|r|^0), \quad (6.11a)$$

$$\Pi_V(t,r)=O^\infty(|r|^{-1-\epsilon}). \quad (6.11b)$$

As

$$\int_{-\infty}^{\infty}dr(\Pi_{\widetilde{\Gamma}}\dot{\widetilde{\Gamma}}-\Pi_V\dot{V})=-\tfrac{1}{2}\dot{\overline{p}}\int_{-\infty}^{\infty}dr\Pi_V+\frac{d}{dt}\int_{-\infty}^{\infty}dr\Pi_{\widetilde{\Gamma}}\widetilde{\Gamma}, \quad (6.12)$$

the transformation to the chart $(\overline{m},\widetilde{m},V(r),\overline{p},\widetilde{p},\Pi_V(r))$ is not canonical as it stands. However, it becomes canonical after the first term on the right-hand side of (6.12) is absorbed into the constraint term by writing

$$N^V:=-\widetilde{N}+\tfrac{1}{2}\dot{\overline{p}} \quad (6.13)$$

and regarding N^V as a new Lagrange multiplier. As the equations of motion imply $\dot{\overline{p}}=0$, the falloff of N^V is

$$N^V=\pm N_\pm+O^\infty(|r|^{-\epsilon}). \quad (6.14)$$

Dropping the integral of a total derivative, and including S_{R}, we finally obtain the action

$$S=\int dt(\overline{p\dot{m}}+\widetilde{p}\dot{\widetilde{m}})+\int dt\int_{-\infty}^{\infty}dr(\Pi_V\dot{V}+\Pi_{\mathsf{R}}\dot{\mathsf{R}}-N^V\Pi_V$$

$$-N^{\mathsf{R}}\Pi_{\mathsf{R}}). \quad (6.15)$$

All the variables in the action (6.15) have a transparent geometrical meaning. From (6.3a), (6.3c), (6.7a), and (6.7c), we see that $\overline{m}$ and $\widetilde{m}$ are respectively equal to the variables $\overline{\mathbf{m}}$ and $\widetilde{\mathbf{m}}$ introduced in Sec. IV. Similarly, using (6.1), we see that $\overline{p}$ and $\widetilde{p}$ can be interpreted as the time-independent initial values of the variables $\overline{\mathbf{p}}$ and $\widetilde{\mathbf{p}}$ introduced in Sec. IV. As for the pure gauge degrees of freedom, R is the curvature radius, and equation (6.10a) shows that V is the Eddington-Finkelstein time. The action (6.15) therefore provides a natural generalization of the vacuum action given in Eq. (149) of Ref. [10].

We have here assumed that the shell history does not lie on a horizon. This assumption can be relaxed, in a suitable limiting sense, by performing on the coordinates $(\overline{m},\widetilde{m},\overline{p},\widetilde{p})$ transformations analogous to those given for the coordinates $(\overline{\mathbf{m}},\widetilde{\mathbf{m}},\overline{\mathbf{p}},\widetilde{\mathbf{p}})$ in Sec. IV.

VII. $\mathbb{R}^3$ SPATIAL TOPOLOGY

In this section we consider the canonical transformation and Hamiltonian reduction for spatial topology $\mathbb{R}^3$. For concreteness, we take the evolution of the spatial hypersurfaces at the single spacelike infinity to be prescribed as in Sec. II. It will be seen that the reduced phase space consists of two disconnected components, one for an expanding shell and the other for a collapsing shell. Each component has the topology $\mathbb{R}^2$.

We start from the action principle. In the bulk action (2.6), we take $0<r<\infty$, with the falloff (2.12) as $r\to\infty$. As $r\to 0$, we introduce the falloff

$$\Lambda(t,r)=\Lambda_0+O(r^2), \quad (7.1a)$$

$$R(t,r)=R_1 r+O(r^3), \quad (7.1b)$$

$$P_\Lambda(t,r)=P_{\Lambda_2}r^2+O(r^4), \quad (7.1c)$$

$$P_R(t,r)=P_{R_1}r+O(r^3), \quad (7.1d)$$

$$N(t,r)=N_0+O(r^2), \quad (7.1e)$$

$$N^r(t,r)=N_1^r r+O(r^3), \quad (7.1f)$$

where $\Lambda_0>0$, $R_1>0$, P_{Λ_2}, P_{R_1}, $N_0>0$, and N_1^r are functions of t only. It is straightforward to verify that the falloff (7.1) is consistent with the constraints and preserved by the time evolution. By (3.1a) and (3.2), the falloff (7.1) implies that the mass left of the shell must vanish when the equations of motion hold: $r=0$ is then just the coordinate singularity at the center of hyperspherical coordinates in flat space. The

classical solutions therefore describe a shell with a flat interior, and the spatial topology is $\mathbb{R}^3$. The action appropriate for fixing N_+ is

$$S = S_\Sigma - \int dt N_+ M_+ , \tag{7.2}$$

where S_Σ is given by (2.6) with $0<r<\infty$.

The canonical transformation of Sec. III goes through with the obvious changes. The new action is as in (3.18), except that the integral is from $r=0$ to $r=\infty$ and the term $N_- M_-$ is missing. $G(r)$ and $g(M_+;r)$ are smooth in r and have the same behavior as $r\to+\infty$ as in Sec. III. The falloff of the new fields as $r\to 0$ can be found from (7.1); for example, we have

$$\widetilde{N}(t,r) = -N_0 \Lambda_0 R_1^{-1} + O(r). \tag{7.3}$$

All the new fields remain regular as $r\to 0$. In particular, $M(r)$ tends to zero as $r\to 0$.

The Hamiltonian reduction proceeds as in Sec. IV, with the simplification that the interior mass vanishes. The reduced phase space consists again of two disconnected components, denoted now by $\widetilde{\Gamma}^E_\eta$. We take $g(M_+;r)$ to be as in (4.1) with $M_-=0$, and we solve the constraint (4.2) as in (4.3) and (4.5) with $\mathbf{m}_-=0$. Note that as Π_M has the same sign as $\mathfrak{p}$, equation (4.5) implies $\mathbf{m}_+>0$. We find

$$\mathfrak{p}\dot{\mathfrak{r}} + \int_0^\infty dr[(\Pi_M - \eta G)\dot{M} - \eta \dot{g}] = \mathbf{p}_+ \dot{\mathbf{m}}_+ + \frac{d}{dt}\left(\eta \mathbf{m}_+ \int_0^{\mathfrak{r}} G dr \right), \tag{7.4}$$

where

$$\mathbf{p}_+ := \int_0^\infty dr[\Pi_M \theta(r-\mathfrak{r}) - \eta G - 2\eta \mathbf{m}_+ g_+]. \tag{7.5}$$

Substituting this in the action and dropping the integral of a total derivative, we obtain the reduced action

$$S = \int dt(\mathbf{p}_+ \dot{\mathbf{m}}_+ - N_+ \mathbf{m}_+). \tag{7.6}$$

Thus, the pair $(\mathbf{m}_+, \mathbf{p}_+)$ provides a canonical chart on $\widetilde{\Gamma}^E_\eta$. As Π_M does not have singularities, the definition (7.5) is always good: the chart is global, and the topology of $\widetilde{\Gamma}^E_\eta$ is $\mathbb{R}^2$. The test shell limit can be attached as a smooth boundary with topology $\mathbb{R}$ at $\mathbf{m}_+=0$.

The information about the shell motion is again encoded in the evolution of $\mathbf{p}_+$. Charts that describe the shell motion in the exterior geometry more transparently can be constructed as in Sec. V.

VIII. SUMMARY AND DISCUSSION

In this paper we have analyzed the Hamiltonian structure of spherically symmetric Einstein gravity coupled to an infinitesimally thin null-dust shell. We formulated the theory under Kruskal-like boundary conditions, prescribing the evolution of the spatial hypersurfaces at the two spacelike infinities. We adopted smoothness conditions that made the variational equations distributionally well defined, and equivalent to the Einstein equations for this system.

We then simplified the constraints by a Kuchař-type canonical transformation and performed the Hamiltonian reduction. It was seen that the reduced phase space consists of two disconnected copies of $\mathbb{R}^4$, one for a right-moving shell and the other for a left-moving shell. We found on each component a global canonical chart in which the configuration variables are the Schwarzschild masses on the two sides of the shell, leaving the shell dynamics indirectly encoded in the conjugate momenta. Excluding the special case of a shell straddling a horizon, we found a local canonical chart in which the configuration variables are the shell curvature radius and the interior mass, in an arbitrarily specifiable stationary coordinate system exterior to the shell. In particular, performing a partial reduction and fixing the interior mass to be a prescribed constant, we reproduced a previously known shell Hamiltonian in the spatially flat gauge outside the shell.

We also cast into canonical form the theory in which the evolution at the infinities is freed by introducing parametrization clocks. We found on the unreduced phase space a global canonical chart in which the physical degrees of freedom and the pure gauge degrees of freedom are completely decoupled, and we identified the pure gauge configuration variables in this chart as the Eddington-Finkelstein time and the curvature radius. Finally, we adapted the analysis to the spatial topology $\mathbb{R}^3$, which has just one infinity, and for which the spacetime inside the shell is flat. Expectedly, the reduced phase space for this spatial topology turned out to consist of two disconnected copies of $\mathbb{R}^2$, one for an expanding shell and the other for a collapsing shell.

In addition to the Kruskal spatial topology $S^2\times\mathbb{R}$ and the Euclidean spatial topology $\mathbb{R}^3$, yet another spatial topology of interest would be that of the $\mathbb{RP}^3$ geon [51], $\mathbb{RP}^3\backslash\{\text{a point at infinity}\}$. As the reduced phase space of the vacuum theory with the $\mathbb{RP}^3$ geon topology has dimension two [13], one expects that the reduced phase space with a null shell would have dimension four. Indeed, this is the conclusion reached under a technically slightly different but qualitatively similar falloff in Ref. [37], by first performing a Hamiltonian reduction for a massive dust shell and then taking the zero rest mass limit. It does not seem straightforward to adapt the canonical transformation of Sec. III to $\mathbb{RP}^3$ geon topology, however. An $\mathbb{RP}^3$-geon-type spacetime with a null shell can be mapped to a Kruskal-type spacetime with two null shells, but these two shells must be moving in opposite directions; our canonical transformation, on the other hand, was adapted to only one direction of the shell motion at a time.

A similar issue arises if one wishes to include more than one null-dust shell. One expects our canonical transformations to generalize readily to the case when all the shells are moving in the same direction. Shells moving in different directions would, however, seem to require new methods.

Several steps in our analysis relied crucially on the fact that the shell is null. This issue appears first in the consistency of the ADM equations of motion in Sec. II. In a fixed background geometry, the equations obtained by varying the

action (2.6) with respect to the shell variables must, by construction, be equivalent to the geodesic equation for the shell. In our dynamical equations (2.9), the pair consisting of (2.9e) and (2.9f), if interpreted individually on each side of the shell, must therefore be equivalent to the null geodesic equation. The reason why the potentially ambiguous equation (2.9f) turns out to be unambiguous is precisely that the junction is along a null hypersurface, and this hypersurface is geodesic in the geometries on both sides of the junction.

Next, the fact that the shell history is null led us to the Eddington-Finkelstein time as a spacetime function that is sufficiently smooth to provide an acceptable momentum conjugate to $M(r)$. Finally, in Sec. V, the null character of the shell history made it possible to leave the interior canonical pair $(\mathbf{m}_-,\mathbf{p}_-)$ untouched in the canonical transformation from $(\mathbf{m}_+,\mathbf{p}_+)$ to $(\hat{r},\hat{p})$. This is because the null history, when viewed from the exterior geometry, does not contain information about the interior mass, beyond the statement that $\mathbf{m}_-<\mathbf{m}_+$.

These special properties of a null shell suggest that our analysis may not be immediately generalizable to timelike shells. For example, for a dust shell with a positive rest mass, already the consistency of the ADM equations of motion fails under our smoothness assumptions: the variational equations corresponding to (2.8) and (2.9) only become consistent if the right-hand side in the counterpart of (2.9f) is by hand interpreted as its average over the two sides of the shell [37]. However, new avenues may open if one relaxes the assumption that the variations of the geometry and matter be independent. Recent progress in this direction has been made by Hájíček and Kijowski [52–54].

The work in this paper has been purely classical. One may, however, hope that our canonical charts on the reduced phase space will prove useful for quantizing the system. In the spatially flat gauge outside the shell, the quantization of the shell variables with fixed interior mass was introduced as a model for Hawking radiation with back-reaction in Ref. [30], and the same approach was applied to related black holes in Refs. [31, 34]. Our results provide the tools for a similar analysis in an arbitrarily specifiable stationary gauge outside the shell. Whether this freedom in the gauge choice can be utilized to a physically interesting end remains to be seen. One may also wish to explore quantizations based on the global canonical charts in which the dynamics is simpler but the spacetime picture more hidden. This might shed light on the analogous question of quantizing in a dynamically simple but geometrically nontransparent canonical chart in the context of a two-dimensional dilatonic gravity theory coupled to scalar fields [55]. We leave these questions subject to future work.

ACKNOWLEDGMENTS

We would like to thank Tevian Dray, Petr Hájíček, Jerzy Kijowski, Karel Kuchař, Charlie Misner, Eric Poisson, and Stephen Winters for discussions. This work was supported in part by NSF grants PHY94-08910, PHY94-21849, and PHY95-07740.

APPENDIX A: HAMILTONIAN EQUATIONS OF MOTION AT THE SHELL

In this appendix we isolate the independent information that the Hamiltonian equations of motion, (2.8) and (2.9), contain at the shell. It will be shown in Appendices B and C that when this information is combined to Einstein's equations away from the shell, we unambiguously recover the correct junction conditions for general relativity coupled to a null-dust shell.

To begin, we note that equations (2.8) and all save the last one of equations (2.9) have an unambiguous distributional interpretation. The constraint equations (2.8) contain explicit delta-functions in r from the matter contribution and implicit delta-functions in R'' and P_Λ'. The right-hand sides of (2.9a) and (2.9b) contain at worst finite discontinuities, and the right-hand sides of (2.9c) and (2.9d) contain at worst delta-functions; this is consistent with the left-hand sides of (2.9a)–(2.9d), recalling that the loci of nonsmoothness in Λ, R, P_Λ and P_R may evolve smoothly in t. Wherever explicit or implicit delta-functions appear, they are multiplied by continuous functions of r. The only potentially troublesome equation is therefore (2.9f): the right-hand side is a combination of spatial derivatives evaluated at the shell, but our assumptions allow these derivatives to be discontinuous.

If f stands for any of our metric functions that may be discontinuous at the shell, we define

$$\Delta f := \lim_{\epsilon\to 0_+}[f(\mathfrak{r}+\epsilon)-f(\mathfrak{r}-\epsilon)]. \tag{A1}$$

The delta-contributions to f' and $\dot{f}$ at the shell can then be written respectively as $(\Delta f)\delta(r-\mathfrak{r})$ and $-\dot{\mathfrak{r}}(\Delta f)\delta(r-\mathfrak{r})$. With this notation, the constraint equations (2.8) at the shell read

$$\Delta R' = -\eta\mathfrak{p}/\hat{R}, \tag{A2a}$$

$$\Delta P_\Lambda = -\mathfrak{p}/\hat{\Lambda}, \tag{A2b}$$

and the delta-contributions in the dynamical equations (2.9c) and (2.9d) at the shell read

$$-\dot{\mathfrak{r}}\Delta P_\Lambda = \frac{\eta\mathfrak{p}\hat{N}}{\hat{\Lambda}^2}+\widehat{N^r}\Delta P_\Lambda, \tag{A3a}$$

$$-\dot{\mathfrak{r}}\Delta P_R = -\frac{\hat{N}\Delta R'+\hat{R}\Delta N'}{\hat{\Lambda}}+\widehat{N^r}\Delta P_R. \tag{A3b}$$

The full set of equations at the shell therefore consists of (2.9e), (2.9f), (A2), and (A3). Of these, all except (2.9f) are manifestly well defined.

Two of the six equations are easily seen to be redundant. First, inserting ΔP_Λ from (A2b) into (A3a) yields an equation that is proportional to (2.9e) by the factor $\mathfrak{p}/\hat{\Lambda}$. Equation (A3a) can therefore be dropped. Second, by continuity of the metric, we observe that $\hat{R}(t)=R(t,\mathfrak{r}(t))$ is well defined for all t, and so is its total time derivative, given by

$$\dot{\hat{R}} = [\dot{R} + \dot{\mathfrak{r}} R']\hat{}\,. \tag{A4}$$

The individual terms on the right-hand side of (A4) are not continuous at the shell, but the left-hand side shows that the sum must be, and we obtain

$$\Delta \dot{R} = -\dot{\mathfrak{r}} \Delta R'. \tag{A5}$$

An entirely similar reasoning leads to counterparts of (A5) with R replaced by any metric function that is continuous in r. Using (A5) and (2.9e), equation (2.5b) gives $\Delta P_\Lambda = \eta \hat{R}(\Delta R')/\hat{\Lambda}$. This shows that the two equations in (A2) are equivalent, and we can drop (A2b).

To simplify (A3b), we evaluate ΔP_R from (2.5b) and eliminate $\dot{R}$ and $\dot{\Lambda}$ using (A5) and its counterpart for Λ. Using (2.9e), the result can be arranged to read

$$0 = \Delta[(v_a v^a)'], \tag{A6}$$

where the vector field v^a is defined by

$$v^t = 1, \tag{A7a}$$

$$v^r = \dot{\mathfrak{r}}, \tag{A7b}$$

both at the shell and away from the shell. At the shell, v^a coincides with the shell history tangent vector ℓ^a (2.10), by virtue of the equation of motion (2.9e). Through standard manipulations, (A6) can be brought to the form

$$0 = \Delta[v_b v^a \nabla_a (\partial_r)^b], \tag{A8}$$

where ∇_a is the spacetime covariant derivative.

The information in the Hamiltonian equations of motion at the shell is therefore captured by the set consisting of (2.9e), (2.9f), (A2a), and (A8).

In Appendices B and C we combine these four equations to the fact that away from the shell, equations (2.8) and (2.9) are equivalent to Einstein's equations and thus make the geometry locally Schwarzschild. As noted in subsection II B, equation (2.9e) implies that the shell history is null. We therefore only need to examine two qualitatively different cases, according to whether or not the shell history lies on a horizon. The results, derived respectively in Appendices B and C, are summarized here in the following two paragraphs:

When the shell history does not lie on a horizon, the continuity of R across the shell completely determines the geometry. Equation (A8) reduces to an identity, and the combination of derivatives on the right-hand side of (2.9f) is continuous at the shell. Equation (2.9f) becomes then well defined. With $\mathfrak{p}$ given by (A2a), equation (2.9f) reduces to an identity.

When the shell history lies on a horizon, the masses on the two sides must agree. Equation (A8) now implies that the soldering along the junction is affine. The combination of derivatives on the right-hand side of (2.9f) is then continuous at the shell, and equation (2.9f) becomes well defined. With $\mathfrak{p}$ given by (A2a), equation (2.9f) reduces to an identity.

APPENDIX B: EQUATIONS OF MOTION FOR A NONSTATIC SHELL

In this appendix we verify the claims in the penultimate paragraph of Appendix A. For concreteness, and without loss of generality, we may assume that the shell history lies right of the horizon that the shell does not cross. The geometry is then as in Fig. 1 for $\eta = -1$, and its time inverse for $\eta = 1$.

On each side of the shell, we introduce the Eddington-Finkelstein coordinates,

$$ds^2 = -F dV^2 - 2\eta dV dR + R^2 d\Omega^2, \tag{B1a}$$

$$F = 1 - 2M/R, \tag{B1b}$$

where M is the Schwarzschild mass. To avoid cluttering the notation, we suppress indices that would distinguish the coordinate patches on the two sides of the shell. Wherever ambiguous quantities are encountered [such as in equations (B4) below], the equations are understood to hold individually on each side of the shell.

The coordinates (t,r) of Sec. II can be embedded in the metric (B1) as $V = V(t,r)$ and $R = R(t,r)$, independently on each side of the shell. We obtain

$$g_{tt} = -F\dot{V}^2 - 2\eta \dot{V}\dot{R}, \tag{B2a}$$

$$g_{rr} = -FV'^2 - 2\eta V' R', \tag{B2b}$$

$$g_{tr} = -F\dot{V}V' - \eta(\dot{V}R' + V'\dot{R}). \tag{B2c}$$

As the surfaces of constant t are spacelike, $\eta V' < 0$ everywhere. Expressing the ADM variables in terms of the metric components and using (B2), we find

$$\frac{\eta N}{\Lambda} - N^r = -\frac{\dot{V}}{V'}. \tag{B3}$$

As in Sec. II, the shell history is written as $r = \mathfrak{r}(t)$, and we write $\hat{R}(t) := R(t, \mathfrak{r}(t))$. We also write, independently on each side of the shell, $\hat{V}(t) := V(t, \mathfrak{r}(t))$, and similarly for $\dot{\hat{R}}$, $\widehat{R'}$, $\dot{\hat{V}}$, $\widehat{V'}$, and so on. We then have, independently on each side of the shell,

$$\dot{\hat{R}} = \dot{\hat{R}} + \dot{\mathfrak{r}}\widehat{R'}, \tag{B4a}$$

$$\dot{\hat{V}} = \dot{\hat{V}} + \dot{\mathfrak{r}}\widehat{V'}. \tag{B4b}$$

With these preliminaries, we turn to the shell equations of motion. First, equation (2.9e) implies, with the help of (B3) and (B4b), that $\dot{\hat{V}} = 0$. The shell history is therefore a hypersurface of constant V, independently on each side. These equations also imply that $\dot{\hat{V}}/\widehat{V'}$ is unambiguous and

$$\dot{\mathfrak{r}} = -\dot{\hat{V}}/\widehat{V'}. \tag{B5}$$

Equations (B2b) and (B2c) yield, after eliminating $\dot{\hat{V}}$ and $\dot{\hat{R}}$ with the help of (B4a) and (B5), the relation

$$\eta \widehat{V'} \dot{\hat{R}} = -\dot{\mathfrak{r}}\widehat{g_{rr}} - \widehat{g_{tr}}. \tag{B6}$$

As the right-hand side of (B6) is unambiguous, and as $\dot{\hat{R}} \neq 0$, (B6) implies that $\widehat{V'}$ is unambiguous. Thus, both $\widehat{V'}$ and $\hat{\dot{V}}$ are unambiguous.

Consider next the constraint (A2a). As $\widehat{V'}$ and $\widehat{g_{rr}}$ are unambiguous, equation (B2b) implies $\Delta R' = -\frac{1}{2}\eta \widehat{V'} \Delta F$. Using (B1b), the constraint (A2a) becomes

$$\mathfrak{p} = -\widehat{V'} \Delta M. \tag{B7}$$

Consider then equation (2.9f). Using (B5) and the relation $\dot{\widehat{V'}} = \hat{\dot{V}} + \dot{\mathfrak{r}} \widehat{V''}$, a straightforward calculation yields

$$\left[\left(\frac{\dot{V}}{V'} \right)' \right]^{\wedge} = \frac{\dot{\widehat{V'}}}{\widehat{V'}}. \tag{B8}$$

As the right-hand side of (B8) is unambiguous, equations (B3) and (B8) show that the right-hand side of (2.9f) is unambiguous. Further, when (B7) holds, it is seen that (2.9f) is identically satisfied.

What remains is equation (A8). In the coordinates (B1) we have, again independently on the two sides of the shell, $\widehat{v^a} = (0, \widehat{v^R}, 0, 0)$, and

$$[v_b v^a \nabla_a (\partial_r)^b]^{\wedge} = -\eta [(v^R)^2 (\partial_r)^V{}_{,R}]^{\wedge}. \tag{B9}$$

As $\widehat{v^R} = \dot{\hat{R}}$, $\widehat{v^R}$ is unambiguous. As $\widehat{(\partial_r)^V} = \widehat{V'} \widehat{(\partial_r)^r} = \widehat{V'}$, we see that $\widehat{(\partial_r)^V}$ is unambiguous. As the vector field denoted on each side by $\partial/\partial R$ is continuous at the shell and tangent to the shell history, $[(\partial_r)^V{}_{,R}]^{\wedge}$ is unambiguous. Therefore, the right-hand side of (B9) is unambiguous, and equation (A8) is identically satisfied.

APPENDIX C: EQUATIONS OF MOTION FOR A STATIC SHELL

In this appendix we verify the claims in the last paragraph of Appendix A. For concreteness, and without loss of generality, we may take $\eta = -1$, so that the shell is moving to the left, and the geometry is as in Fig. 2.

On each side of the shell, we introduce the Kruskal null coordinates,

$$ds^2 = -G du dv + R^2 d\Omega^2, \tag{C1a}$$

$$G = (32M^3/R) \exp(-R/2M), \tag{C1b}$$

$$-uv = \left(\frac{R}{2M} - 1 \right) \exp(R/2M), \tag{C1c}$$

where M is the common value of the Schwarzschild mass. When there is a need to distinguish the two coordinate patches, we write the coordinates as $(u_\pm, v_\pm)$, with the upper (lower) sign referring to the patch on the right (left). The ranges of the coordinates are $v_+ > 0$ and $v_- < 0$, with $-\infty < u_\pm < \infty$, and the shell history lies at the common horizon at $v_\pm = 0$. When the index is suppressed, equations containing ambiguous terms are understood to hold individually on each side of the shell.

Embedding the coordinates (t,r) in the metric (C1) as $u = u(t,r)$ and $v = v(t,r)$, independently on each side of the shell, we obtain

$$g_{tt} = -G \dot{u} \dot{v}, \tag{C2a}$$

$$g_{rr} = -G u' v', \tag{C2b}$$

$$g_{tr} = -\tfrac{1}{2} G (\dot{u} v' + u' \dot{v}). \tag{C2c}$$

As the surfaces of constant t are spacelike, $v' > 0$ everywhere. Expressing the ADM variables in terms of the metric components and using (C2), we find

$$\frac{N}{\Lambda} + N^r = \frac{\dot{v}}{v'}. \tag{C3}$$

As above, we introduce the quantities $\hat{u}$, $\hat{\dot{u}}$, $\widehat{u'}$, and so on, and similarly for v. The counterparts of equations (B4) read

$$\hat{\dot{u}} = \hat{\dot{u}} + \dot{\mathfrak{r}} \widehat{u'}, \tag{C4a}$$

$$\hat{\dot{v}} = \hat{\dot{v}} + \dot{\mathfrak{r}} \widehat{v'}. \tag{C4b}$$

Equation (2.9e) then implies, with the help of (C3) and (C4b), that $\hat{\dot{v}} = 0$, $\hat{\dot{v}}/\widehat{v'}$ is unambiguous, and

$$\dot{\mathfrak{r}} = -\hat{\dot{v}}/\widehat{v'}. \tag{C5}$$

Consider next equation (A8). In the coordinates (C1) we have, independently on the two sides of the shell, $\widehat{v^a} = (\widehat{v^u}, 0, 0, 0)$, and

$$[v_b v^a \nabla_a (\partial_r)^b]^{\wedge} = [(v^u)^2 (\partial_r)_{u,u}]^{\wedge}. \tag{C6}$$

Equation (A8) therefore reads

$$(v^{u_+})^2 (\partial_r)_{u_+, u_+} = (v^{u_-})^2 (\partial_r)_{u_-, u_-}, \tag{C7}$$

at the junction $v_\pm = 0$. Writing $v^{u_-} = (du_-/du_+) v^{u_+}$, $(\partial_r)_{u_-} = (du_+/du_-)(\partial_r)_{u_+}$, and $\partial_{u_-} = (du_+/du_-) \partial_{u_+}$, we obtain $d^2 u_-/du_+^2 = 0$. This means that at the junction $v_\pm = 0$ we have

$$u_+ = \alpha u_- + \beta, \tag{C8}$$

where α and β are constants and $\alpha > 0$. As the Kruskal coordinates are affine parameters along the horizons, this means that the soldering of the two geometries along the common horizon is affine.

Consider next the constraint (A2a). From (C1c) we have $\widehat{R'} = -2M \hat{u} \widehat{v'}$. The constraint (A2a) therefore reads

$$\mathfrak{p} = -4M^2 \Delta(uv'). \tag{C9}$$

Equations (C2b) and (C2c) yield, after eliminating $\hat{\dot{v}}$ and $\hat{\dot{u}}$ with the help of (C4a) and (C5), the relation

$$8M^2\widehat{v'}\dot{\hat{u}} = -\dot{\mathfrak{r}}\widehat{g_{rr}} - \widehat{g_{tr}}. \tag{C10}$$

As the right-hand side of (C10) is unambiguous, $\widehat{v'}\dot{\hat{u}}$ is unambiguous. The affine relation (C8) implies $\dot{\widehat{u_+}} = \alpha\dot{\widehat{u_-}}$, and hence

$$\widehat{v'_+} = \alpha^{-1}\widehat{v'_-}. \tag{C11}$$

Hence $\Delta(uv') = \beta\widehat{v'_+}$, and equation (C9) takes the form

$$\mathfrak{p} = -4M^2\beta\widehat{v'_+}. \tag{C12}$$

As $\mathfrak{p} < 0$ by assumption and $\widehat{v'_+} > 0$, we have $\beta > 0$. This means that the right-hand-side bifurcation two-sphere occurs earlier on the history than the left-hand-side bifurcation two-sphere, as shown in Fig. 2.

Consider finally equation (2.9f). Using (C5) and proceeding as with (B8), we find

$$\left[\left(\frac{\dot{v}}{v'}\right)'\right]\hat{} = \frac{\dot{\widehat{v'}}}{\widehat{v'}}. \tag{C13}$$

By (C11), the right-hand side of (C13) is unambiguous. Equations (C3) and (C13) then show that the right-hand side of (2.9f) is unambiguous. When (C12) holds, it is seen that (2.9f) is identically satisfied.

[1] I. H. Redmount, Prog. Theor. Phys. **73**, 1401 (1985).
[2] T. Dray and G. 't Hooft, Nucl. Phys. **B253**, 173 (1985).
[3] T. Dray and G. 't Hooft, Commun. Math. Phys. **99**, 613 (1985).
[4] C. J. S. Clarke and T. Dray, Class. Quantum Grav. **4**, 265 (1987).
[5] C. Barrabes and W. Israel, Phys. Rev. D **43**, 1129 (1991).
[6] B. K. Berger, D. M. Chitre, V. E. Moncrief, and Y. Nutku, Phys. Rev. D **8**, 3247 (1973).
[7] W. G. Unruh, Phys. Rev. D **14**, 870 (1976).
[8] T. Thiemann and H. A. Kastrup, Nucl. Phys. **B399**, 211 (1993).
[9] H. A. Kastrup and T. Thiemann, Nucl. Phys. **B425**, 665 (1994).
[10] K. V. Kuchař, Phys. Rev. D **50**, 3961 (1994).
[11] T. Thiemann, Int. J. Mod. Phys. D **3**, 293 (1994).
[12] T. Thiemann, Nucl. Phys. **B436**, 681 (1995).
[13] J. Louko and B. F. Whiting, Phys. Rev. D **51**, 5583 (1995).
[14] M. Cavaglià, V. de Alfaro, and A. T. Filippov, Int. J. Mod. Phys. D **4**, 661 (1995).
[15] M. Cavaglià, V. de Alfaro, and A. T. Filippov, Int. J. Mod. Phys. D **5**, 227 (1996).
[16] S. R. Lau, Class. Quantum Grav. **13**, 1541 (1996).
[17] D. Marolf, Class. Quantum Grav. **13**, 1871 (1996).
[18] J. Louko and J. Mäkelä, Phys. Rev. D **54**, 4982 (1996).
[19] J. Louko and S. N. Winters-Hilt, Phys. Rev. D **54**, 2647 (1996).
[20] J. Gegenberg and G. Kunstatter, Phys. Rev. D **47**, R4192 (1993).
[21] J. Gegenberg, G. Kunstatter, and D. Louis-Martinez, Phys. Rev. D **51**, 1781 (1995).
[22] D. Louis-Martinez and G. Kunstatter, Phys. Rev. D **52**, 3494 (1995).
[23] T. Brotz and C. Kiefer, Phys. Rev. D **55**, 2186 (1997).
[24] R. Laflamme, in *Origin and Early History of the Universe: Proceedings of the 26th Liège International Astrophysical Colloquium (1986)*, edited by J. Demaret (Université de Liège, Institut d'Astrophysique, 1987); R. Laflamme, Ph.D. thesis, University of Cambridge, 1988; B. F. Whiting and J. W. York, Phys. Rev. Lett. **61**, 1336 (1988); H. W. Braden, J. D. Brown, B. F. Whiting, and J. W. York, Phys. Rev. D **42**, 3376 (1990); J. J. Halliwell and J. Louko, *ibid.* **42**, 3997 (1990); G. Hayward and J. Louko, *ibid.* **42**, 4032 (1990); J. Louko and B. F. Whiting, Class. Quantum Grav. **9**, 457 (1992); J. Melmed and B. F. Whiting, Phys. Rev. D **49**, 907 (1994); S. Carlip and C. Teitelboim, Class. Quantum Grav. **12**, 1699 (1995); S. Carlip and C. Teitelboim, Phys. Rev. D **51**, 622 (1995); G. Oliveira-Neto, *ibid.* **53**, 1977 (1996).
[25] V. P. Frolov, Zh. Eksp. Teor. Fiz. **66**, 813 (1974) [Sov. Phys. JETP **39**, 393 (1974)].
[26] V. A. Berezin, N. G. Kozmirov, V. A. Kuzmin, and I. I. Tkachev, Phys. Lett. B **212**, 415 (1988).
[27] W. Fischler, D. Morgan, and J. Polchinski, Phys. Rev. D **42**, 4042 (1990).
[28] P. Hájíček, Commun. Math. Phys. **150**, 545 (1992).
[29] P. Hájíček, B. S. Kay, and K. V. Kuchař, Phys. Rev. D **46**, 5439 (1992).
[30] P. Kraus and F. Wilczek, Nucl. Phys. **B433**, 403 (1995).
[31] P. Kraus and F. Wilczek, Nucl. Phys. **B437**, 231 (1995).
[32] K. Nakamura, Y. Oshiro, and A. Tomimatsu, Phys. Rev. D **53**, 4356 (1996).
[33] A. D. Dolgov and I. B. Khriplovich, Phys. Lett. B **400**, 12 (1997).
[34] E. Keski-Vakkuri and P. Kraus, Nucl. Phys. **B491**, 249 (1997).
[35] P. Hájíček and J. B. Bičák, Phys. Rev. D **56**, 4706 (1997).
[36] S. J. Kolitch and D. M. Eardley, Phys. Rev. D **56**, 4663 (1997).
[37] J. L. Friedman, J. Louko, and S. N. Winters-Hilt, Phys. Rev. D **56**, 7674 (1997).
[38] S. Ansoldi, A. Aurilia, R. Balbinot, and E. Spallucci, Class. Quantum Grav. **14**, 2727 (1997).
[39] F. Lund, Phys. Rev. D **8**, 3247 (1973).
[40] J. D. Romano, ''Spherically Symmetric Scalar Field Collapse: An Example of the Space-time Problem of Time,'' Report UU-REL-95/1/13, gr-qc/9501015.
[41] J. D. Romano, Phys. Rev. D **55**, 1112 (1997).
[42] R. Geroch and J. Traschen, Phys. Rev. D **36**, 1017 (1987).
[43] P. Painlevé, C. R. Acad. Sci. (Paris) **173**, 677 (1921).
[44] A. Gullstrand, Ark. Mat., Astron. Fys. **16**(8), 1 (1922).
[45] W. Israel, in *Three Hundred Years of Gravitation*, edited by S. W. Hawking and W. Israel (Cambridge University Press, Cambridge, 1987), p. 234.
[46] W. Israel, Nuovo Cimento B **44**, 1 (1966).

[47] C. W. Misner, K. S. Thorne, and J. A. Wheeler, *Gravitation* (Freeman, San Francisco, 1973).
[48] C. Teitelboim, Ann. Phys. (N.Y.) **79**, 524 (1973).
[49] M. Henneaux and C. Teitelboim, *Quantization of Gauge Systems* (Princeton University Press, Princeton, NJ, 1992).
[50] R. Beig and N. Ó Murchada, Ann. Phys. (N.Y.) **174**, 463 (1987).
[51] J. L. Friedman, K. Schleich, and D. M. Witt, Phys. Rev. Lett. **71**, 1486 (1993); **75**, 1872(E) (1995).
[52] P. Hájíček and J. Kijowski, Phys. Rev. D **57**, 914 (1998).
[53] P. Hájíček, Phys. Rev. D **57**, 936 (1998).
[54] P. Hájíček and J. Kijowski (private communication).
[55] K. V. Kuchař, J. D. Romano, and M. Varadarajan, Phys. Rev. D **55**, 795 (1997).